Figure 1. Pathogenesis in immunocompetent mice with persistent HCV expression. (**A**) Structure of CN2-29$^{(+/-)}$/MxCre$^{(+/-)}$ and the Cre-mediated activation of the transgene unit. R6CN2 HCV cDNA was cloned downstream of the CAG promoter, neomycin-resistant gene (*neo*), and poly A (pA) signal flanked by two *loxP* sequences. This cDNA contains the core, E1, E2, and NS2 regions. (**B**) Cre-mediated genomic DNA recombination. After poly(I:C) injection, genomic DNA was extracted from liver tissues and analyzed by quantitative RTD-PCR for Cre-mediated transgenic recombination. The transgene was almost fully recombined in transgenic mouse livers 7 days after the injection. In all cases, n = 3 mice per group. (**C**) HCV core protein expression was sustained for at least 600 days after poly(I:C) injection. (**D**) Immunohistochemical analysis revealed that most hepatocytes expressed the HCV core protein within 6 days after injection. (**E**) Liver sections from CN2-29$^{(+/-)}$/MxCre$^{(+/-)}$ mice after the poly(I:C) injection. Infiltrating lymphocytes (arrows) were observed on days 6 and 180; Hepatocellular carcinoma (HCC) was observed on day 360. In contrast, these pathological changes were not observed in CN2-29$^{(+/-)}$/MxCre$^{(-/-)}$ mice after the injection. The inset image shows abnormal mitosis in a tumor cell. (**F**) Hepatocyte swelling and abnormal architecture of liver-cell cords (silver staining), as well as abnormal glycogen accumulation (PAS staining) were observed on day 90 in CN2-29$^{(+/-)}$/MxCre$^{(+/-)}$ mice. We observed steatosis (oil-red-O staining) on day 180 and, subsequently, fibrosis (Azan staining) on day 480. The scale bars indicate 50 μm.
doi:10.1371/journal.pone.0051656.g001

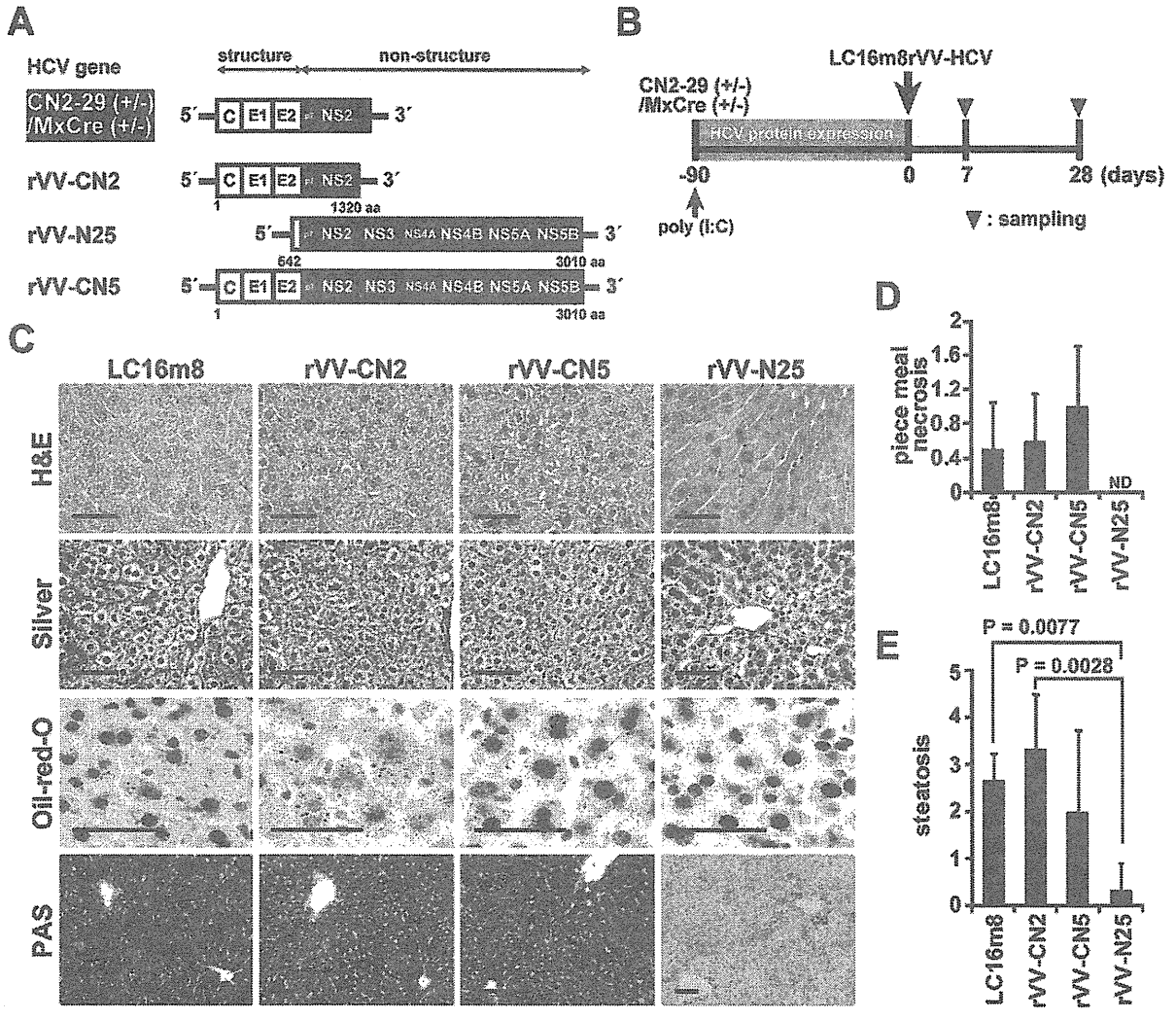

Figure 2. Effects of rVV-HCV treatment on the CN2-29$^{(+/-)}$/MxCre$^{(+/-)}$ mice. (**A**) HCV gene structure in the CN2-29$^{(+/-)}$/MxCre$^{(+/-)}$ mice and recombinant vaccinia viruses (rVV-HCV). MxCre/CN2-29 cDNA contains the core, E1, E2, and NS2 regions. The rVV-CN2 cDNA contains the core, E1, E2, and NS2 regions. The rVV-N25 cDNA contains the NS2, NS3, NS4A, NS4B, NS5A, and NS5B regions. The rVV-CN5 cDNA contains the entire HCV region. (**B**) Four groups of CN2-29$^{(+/-)}$/MxCre$^{(+/-)}$ mice were inoculated intradermally with rVV-CN2, rVV-N25, rVV-CN5, or LC16m8 90 days after the poly(I:C) injection. Blood, liver, and spleen tissue samples were collected 7 and 28 days after the inoculation. (**C**) Liver sections from the four groups of CN2-29$^{(+/-)}$/MxCre$^{(+/-)}$ mice 7 days after the inoculation. The sections were stained with H&E, silver, oil-red-O, or PAS. The scale bars indicate 50 μm. (**D**) Histological evaluation of piecemeal necrosis in the four groups of CN2-29$^{(+/-)}$/MxCre$^{(+/-)}$ mice 7 days after inoculation. (**E**) Histological evaluation of steatosis in the four groups of CN2-29$^{(+/-)}$/MxCre$^{(+/-)}$ mice 7 days after inoculation. Significant relationships are indicated by a P-value.
doi:10.1371/journal.pone.0051656.g002

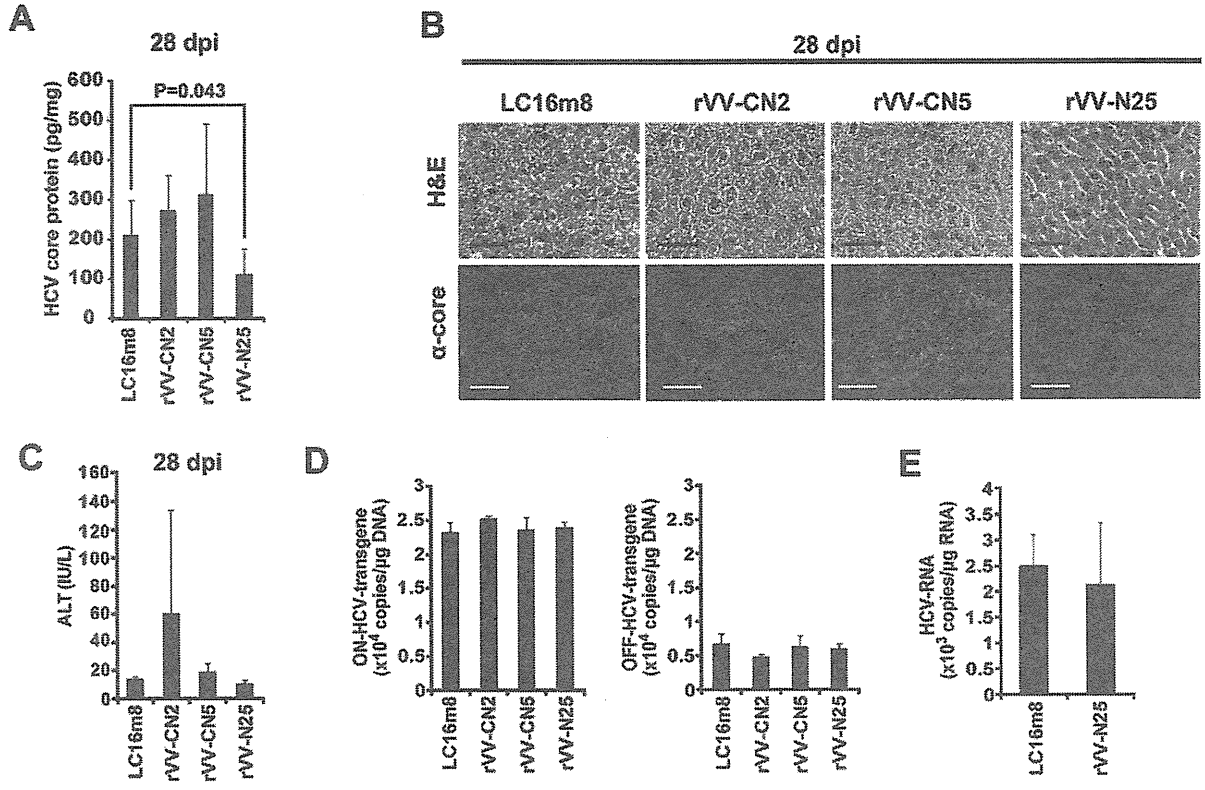

Figure 3. Effects of HCV core protein expression on the livers of CN2-29$^{(+/-)}$/MxCre$^{(+/-)}$ mice inoculated with rVV-HCV. (**A**) Expression of the HCV core protein in the four treatment groups of CN2-29$^{(+/-)}$/MxCre$^{(+/-)}$ mice 28 days after the inoculation. Significant relationships are indicated by a P-value. (**B**) H&E staining and immunohistochemical analysis for HCV core protein in the LC16m8-, rVV-CN2-, rVV-CN5-, or rVV-N25-treated CN2-29$^{(+/-)}$/MxCre$^{(+/-)}$ mice 28 days after the inoculation. Liver sections were stained with the anti-core monoclonal antibody. The scale bars indicate 50 μm. (**C**) Effects of HCV core protein expression on serum ALT levels in the four treatment groups of CN2-29$^{(+/-)}$/MxCre$^{(+/-)}$ mice 28 days after immunization. (**D**) Cre-mediated genomic DNA recombination in the four treatment groups 28 days after immunization. (**E**) Expression of HCV mRNA in the LC16m8- or rVV-N25-treated CN2-29$^{(+/-)}$/MxCre$^{(+/-)}$ mice 28 days after immunization. In all cases, n = 6 mice per group.
doi:10.1371/journal.pone.0051656.g003

ly different in the rVV-N25-treated mice and control mice (Figure 3C); this finding indicated that rVV-N25 treatment did not cause liver injury and that the antiviral effect was independent of hepatocyte destruction.

We hypothesized that the reduction in the levels of HCV core protein in rVV-HCV-treated mice was not caused by cytolytic elimination of hepatocytes that expressed HCV proteins. To investigate this hypothesis, we conducted an RTD-PCR analysis of genomic DNA from liver samples of CN2-29$^{(+/-)}$/MxCre$^{(+/-)}$ mice. The recombined transgene was similar in rVV-N25-treated and control mice 28 days after immunization (Figure 3D). We also measured the expression of HCV mRNA in LC16m8-treated CN2-29$^{(+/-)}$/MxCre$^{(+/-)}$ mice with that in rVV-N25-treated CN2-29$^{(+/-)}$/MxCre$^{(+/-)}$ mice 28 days after immunization; the HCV mRNA levels did not differ between rVV-N25-treated CN2-29$^{(+/-)}$/MxCre$^{(+/-)}$ and control mice (Figure 3E). These results indicated that rVV-N25-induced suppression of HCV core protein expression could be controlled at a posttranscriptional level.

Role of CD4 and CD8 T cells in rVV-N25-treated Mice

Viral clearance is usually associated with CD4 and CD8 T-cell activity that is regulated by cytolytic or noncytolytic antiviral mechanism [14]. To determine whether CD4 or CD8 T-cell activity was required for the reduction in HCV core protein levels in the livers of transgenic mice, we analyzed the core protein levels in CN2-29$^{(+/-)}$/MxCre$^{(+/-)}$ mice immunized with rVV-N25 in the absence of CD4 or CD8 T cells (Figure 4A). As expected, the mice lacking CD4 or CD8 T cells failed to show a reduction in HCV core protein levels (Figure 4B).

However, in mice lacking either CD4 or CD8 T-cells, the pathological changes associated with chronic hepatitis were resolved following rVV-N25 immunization, and the steatosis score of rVV-N25-treated mice was significantly lower than that of control mice (Figures 4C–E). These results indicated that CD4 and CD8 T cells were not responsible for the rVV-N25-induced amelioration of histological findings and that other inflammatory cell types may play an as-yet-unidentified role in the resolution of the pathological changes in these mice.

rVV-N25 Immunization Induced an NS2-specific Activated CD8 T cells Response

Because we found that HCV protein reduction in the liver required CD8 T cells, we tested whether HCV-specific CD8 T cells were present in splenocytes 28 days after immunization. To determine the functional reactivity of HCV-specific CD8$^+$ T cells, we performed a CD107a mobilization assay and intracellular IFN-γ staining. CN2-29 transgenic mice expressed the HCV structural protein and the NS2 region. However, rVV-N25 comprised only

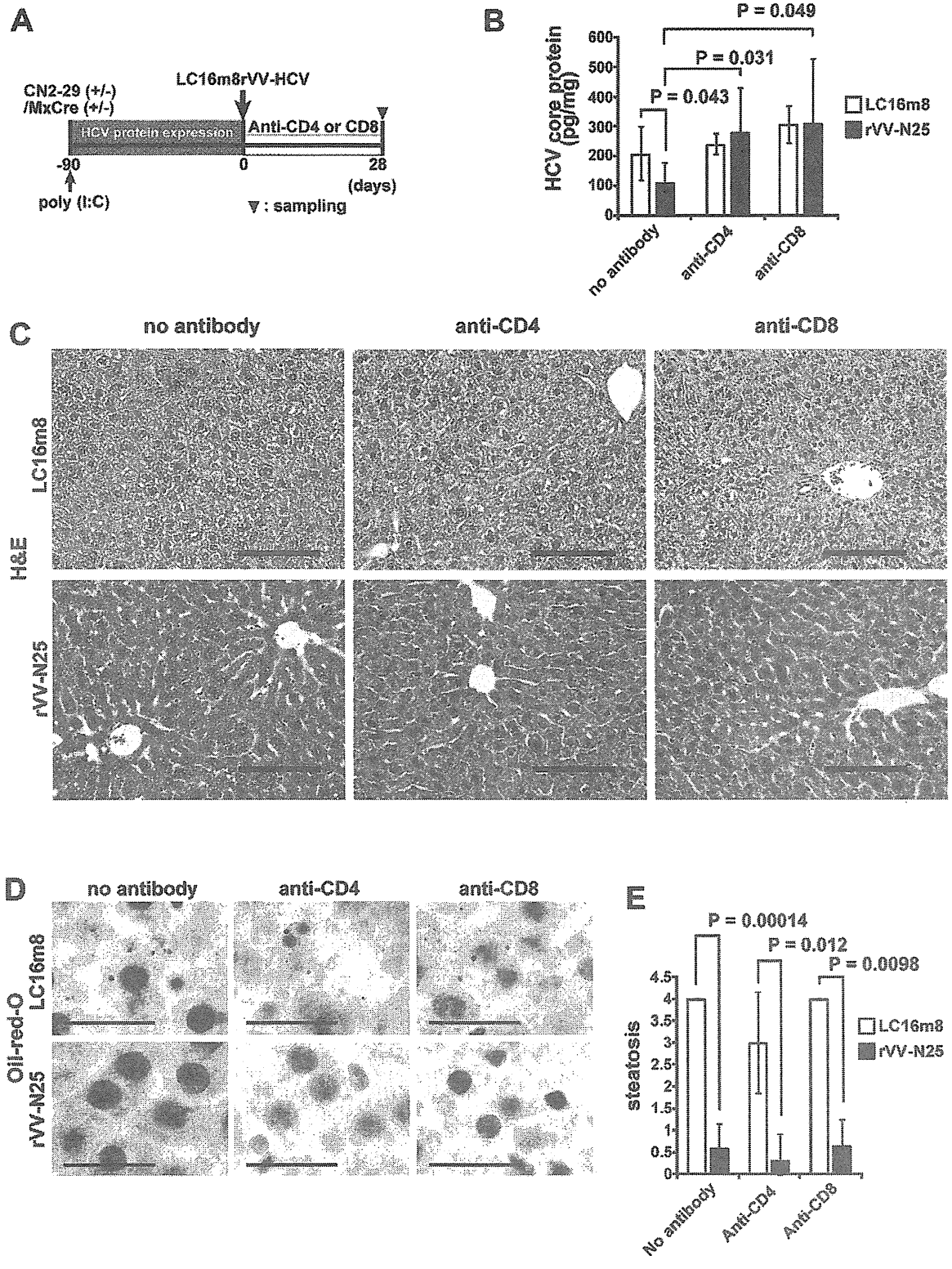

Figure 4. Role of CD4 and CD8 T cells in rVV-N25-treated mice. (**A**) Schematic diagram depicts depletion of CD4 and CD8 T cells via treatment with monoclonal antibodies. (**B**) Comparison of HCV core protein expression in control, CD4-depleted, and CD8-depleted mice 28 days after immunization with LC16m8 or rVV-N25. (**C, D**) Histological analysis of liver samples from CD4-depleted or CD8-depleted CN2-29$^{(+/-)}$/MxCre$^{(+/-)}$ mice

28 days after immunization with LC16m8 or rVV-N25. The scale bars indicate 100 μm (**C**) and 50 μm (**D**). (**E**) Histological evaluation of steatosis in liver samples from CD4-depleted or CD8-depleted CN2-29$^{(+/-)}$/MxCre$^{(+/-)}$ mice 28 days after immunization with LC16m8 or rVV-N25. Significant relationships are indicated by a P-value.
doi:10.1371/journal.pone.0051656.g004

a HCV nonstructural protein. Thus, we focused on the role of the NS2 region as the target for CD8 T cells and generated EL-4 cell lines that expressed the NS2 antigen or the CN2 antigen.

Isolated splenocytes from immunized mice were co-cultured with EL-4CN2 or EL-4NS2 cell lines for 2 weeks and analyzed.

Cytolytic cell activation can be measured using CD107a, a marker of degranulation [15]. The ratio of CD8$^+$CD107a$^+$ cells to all CD8 T cells significantly increased in rVV-N25-treated splenocytes after co-culture with EL-4CN2 or EL-4NS2 ($P<0.05$), whereas splenocytes that had been treated with any other rVV were not detected (Figure 5A, B and C). These results indicated that rVV-N25 treatment increased the frequency of HCV NS2-specific activated CD8 T cells. Consistent with these results, the ratio of CD8$^+$IFN-γ$^+$ cells to all CD8 T cells for rVV-N25-treated mice was also significantly higher than that for mice treated with any other rVV ($P<0.05$). Taken together, these findings indicated that rVV-N25 induced an effective CD8 T-cell immune response and that NS2 is an important epitope for CD8 T cells.

rVV-N25 Immunization Suppressed Inflammatory Cytokines Production

To determine whether rVV-N25 treatment affected inflammatory cytokine production, we measured serum levels of inflammatory cytokines after rVV immunization. The serum levels of these inflammatory cytokines increased in the CN2-29$^{(+/-)}$/MxCre$^{(+/-)}$ mice (Figure 6A, Figure S5). Immunization with rVV-N25 affected serum levels of inflammatory cytokines in CN2-29$^{(+/-)}$/MxCre$^{(+/-)}$ mice and caused a return to the cytokine levels observed in wild-type untreated mice (Figure 6A). In wild-type mice, the cytokine levels remained unchanged after immunization (Figure 6A). These results indicated that inflammatory cytokines were responsible for liver pathogenesis in the transgenic mice.

To test the hypothesis that inflammatory cytokines were responsible for liver pathogenesis in CN2-29$^{(+/-)}$/MxCre$^{(+/-)}$ mice, we administered transgenic mouse serum intravenously into nontransgenic mice. We observed the development of chronic hepatitis in the nontransgenic mice within 7 days after the serum transfer (Figures 6B and C). This finding was consistent with the

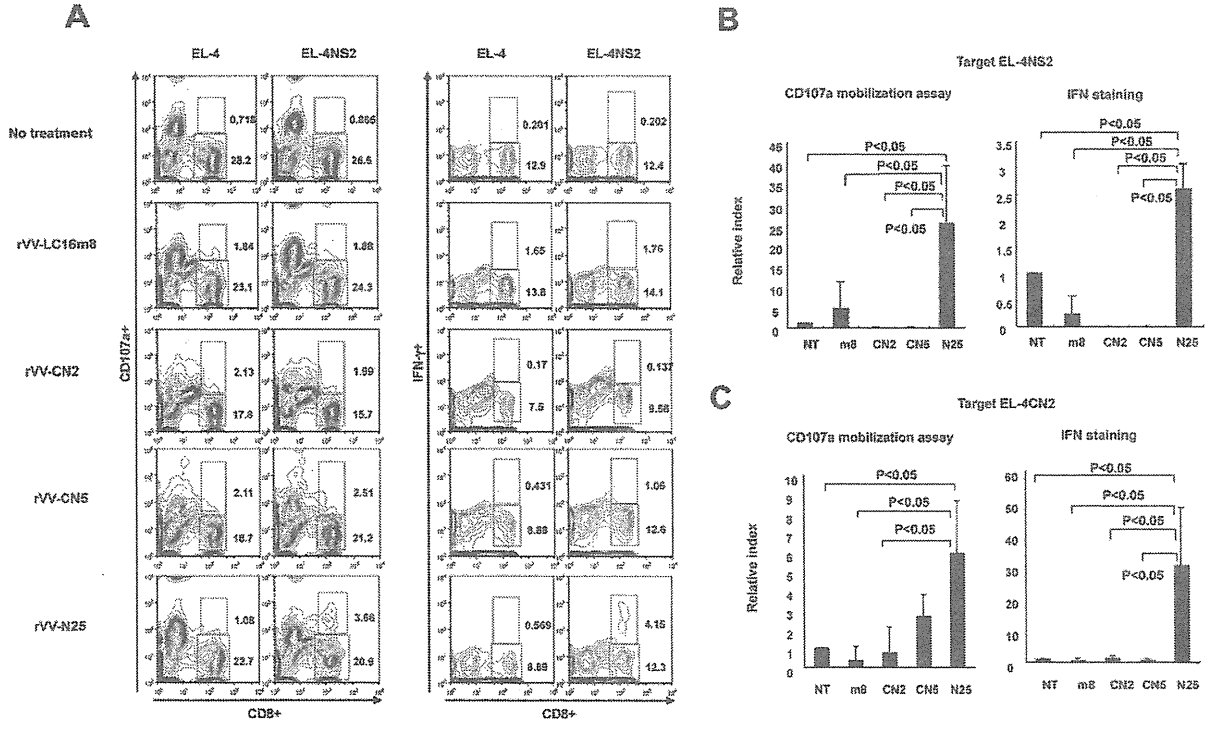

Figure 5. Immunization with rVV-N25 induced CD8 T-cell degranulation, a marker for cytotoxicity, and IFN-γ production. (**A**) The numbers represent the percentage of CD107a positive cells and negative cells (left two columns) and IFN-γ-positive cells and negative cells (right two columns). (**B, C**) The ratio of CD8$^+$IFN-γ$^+$ cells to all CD8 T cells for rVV-N25-treated mice was significantly higher than that for mice treated with any other rVV. Splenocytes (4×10^6 per well) were cultured with EL-4CN2 or EL-4NS2 cell lines in RPMI 1640 complete medium including 3% T-STIM^{TM} with ConA for 2 weeks. Harvested cells were incubated for 4 h with EL-4, EL-4CN2, or EL-4NS2 in combination with PE-labeled anti-CD107a mAb and monensin in RPMI 1640 complete medium with 50 IU/mL IL-2, according to the manufacturer's instruction. After incubation, cell suspensions were washed with PBS, and the cells were further stained with APC-labeled anti-IFN-γ mAb and Pacific blue-labeled anti-CD8 mAb. Harvested cells were stained with anti-CD107a-PE, anti-IFN-γ-APC, or anti-CD8-Pacific blue. Results that are representative of three independent experiments are shown. Significant relationships are indicated by P-value.
doi:10.1371/journal.pone.0051656.g005

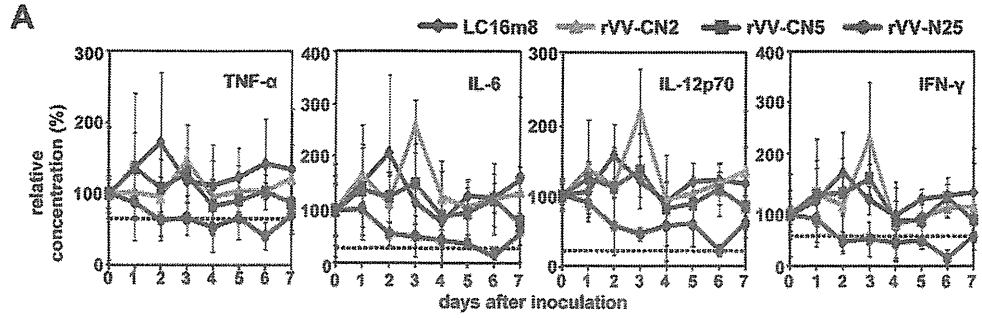
A
LC16m8
rVV-CN2
rVV-CN5
rVV-N25
TNF-α
IL-6
IL-12p70
IFN-γ
relative concentration (%)
days after inoculation

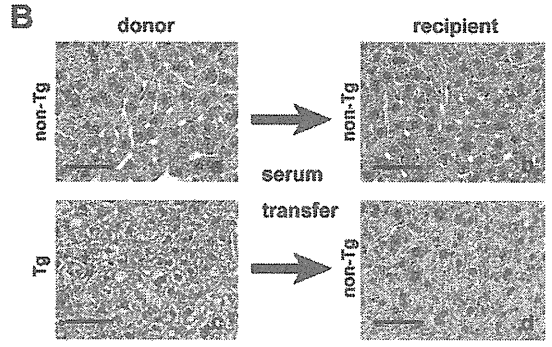
B
donor
recipient
non-Tg
Tg
serum transfer

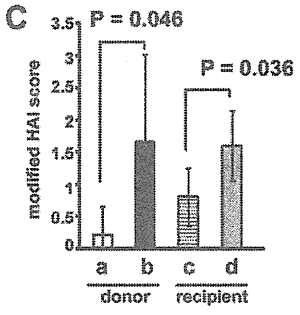
C
P = 0.046
P = 0.036
modified HAI score
a
b
c
d
donor
recipient

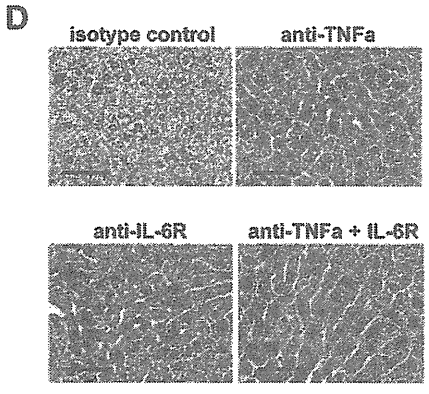
D
isotype control
anti-TNFa
anti-IL-6R
anti-TNFa + IL-6R

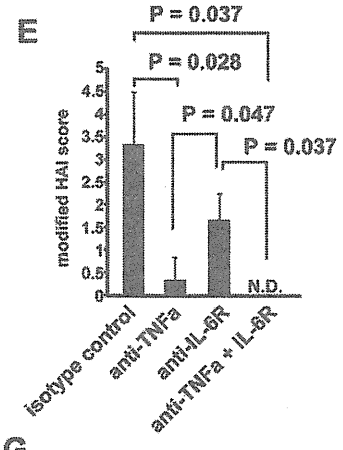
E
P = 0.037
P = 0.028
P = 0.047
P = 0.037
modified HAI score
N.D.
isotype control
anti-TNFa
anti-IL-6R
anti-TNFa + IL-6R

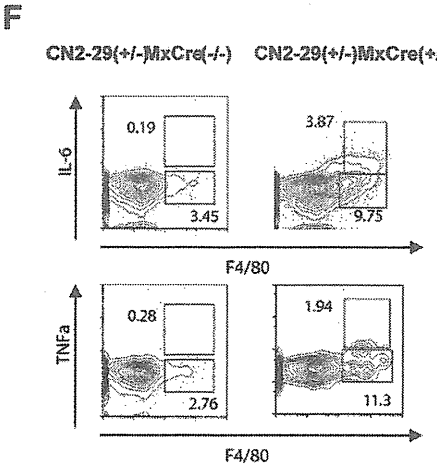
F
CN2-29(+/-)MxCre(-/-)
CN2-29(+/-)MxCre(+/-)
IL-6
TNFa
F4/80
0.19
3.45
3.87
9.75
0.28
2.76
1.94
11.3

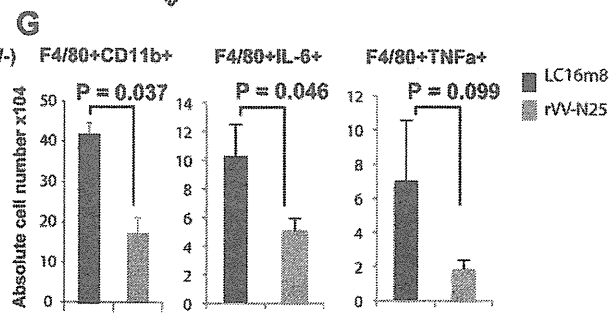
G
F4/80+CD11b+
F4/80+IL-6+
F4/80+TNFa+
P = 0.037
P = 0.046
P = 0.099
Absolute cell number x10⁴
LC16m8
rVV-N25

Figure 6. Immunization with rVV-N25 suppresses serum inflammatory cytokine levels. (**A**) Daily cytokine levels in the serum of CN2-29$^{(+/-)}$/MxCre$^{(+/-)}$ mice during the week following immunization with LC16m8, rVV-CN2, rVV-N25, or rVV-CN5. Values represent means ± SD (n = 3) and reflect the concentrations relative to those measured on day 0. The broken lines indicate the baseline data from wild-type mice. In all cases, n = 6 mice per group. (**B**) Liver sections from CN2-29$^{(+/-)}$/MxCre$^{(+/-)}$ and CN2-29$^{(+/-)}$/MxCre$^{(-/-)}$ mice. (**C**) Histology activity index (HAI) scores of liver samples taken from CN2-29$^{(+/-)}$/MxCre$^{(+/-)}$, or CN2-29$^{(+/-)}$/MxCre$^{(-/-)}$ mice. (**D**) Liver sections from CN2-29$^{(+/-)}$/MxCre$^{(+/-)}$ mice in which TNF-α was neutralized and the IL-6 receptor was blocked. The scale bars indicate 50 μm. (**E**) HAI scores of liver samples taken from CN2-29$^{(+/-)}$/MxCre$^{(+/-)}$ in which TNF-α was neutralized and the IL-6 receptor was blocked. Tg and non-Tg indicate CN2-29$^{(+/-)}$/MxCre$^{(+/-)}$ and CN2-29$^{(+/-)}$/MxCre$^{(-/-)}$, respectively. (F) Macrophages were the main producers of TNF-α and IL-6 in CN2-29$^{(+/-)}$/MxCre$^{(+/-)}$ mice following poly(I:C) injection. (G) Immunization with rVV-N25 reduced the number of macrophages in liver samples from CN2-29$^{(+/-)}$/MxCre$^{(+/-)}$ mice and suppressed TNF-α and IL-6 production from macrophages (Figure 6G). Significant relationships are indicated by a P-value.
doi:10.1371/journal.pone.0051656.g006

hypothesis that inflammatory mediators played a key role in inducing hepatitis. Furthermore, to investigate whether TNF-α and IL-6 played particularly critical roles in the pathogenesis of chronic hepatitis in the transgenic mice, we neutralized TNF-α and blocked the IL-6 receptor in the livers of these mice. As expected, chronic hepatitis did not develop in these mice. (Figure 6D and E).

Next, to determine which cell population(s) produced TNF-α, IL-6, or both during continuous HCV expression in CN2-29$^{(+/-)}$/MxCre$^{(+/-)}$ mice, we isolated intrahepatic lymphocytes (IHLs) and labeled the macrophages (the F4/80^{+} cells) with anti-TNF-α and anti-IL-6 antibodies using an intracellular cytokine detection method. Macrophages in CN2-29$^{(+/-)}$/MxCre$^{(-/-)}$ mice produced small amounts of TNF-α and IL-6, while those in CN2-29$^{(+/-)}$/MxCre$^{(+/-)}$ mice produced much larger amounts of these cytokines (Figure 6F).

Finally, we evaluated whether rVV-N25 treatment affected the number of macrophages, cytokine production by macrophages, or both; specifically, we isolated IHLs from CN2-29$^{(+/-)}$/MxCre$^{(+/-)}$ mice 7 days after immunization with rVV-N25 or with LC16m8. The percentage of macrophages (CD11b^{+}F4/80^{+}) among IHLs and IL-6 production from these macrophages were significantly lower in rVV-N25-treated mice than in control mice (Figure 6G). Though the percentage of TNF-α-producing macrophages was not significantly different in rVV-N25-treated and control mice (P = 0.099), rVV-N25 treatment appeared to suppress these macrophages. These results demonstrated that rVV-N25 had a suppressive effect on activated macrophages, and they indicated that this suppression ameliorated the histological indicators of chronic hepatitis.

Discussion

Various HCV transgenic mouse models have been developed and used to examine immune response to HCV expression and the effects of pathogenic HCV protein on hepatocytes [4,16,17]. However, these transgenic mice develop tolerance to the HCV protein; therefore, examining immune response to HCV protein has been difficult.

To overcome the problem of immune tolerance in mouse models of HCV expression, we developed an HCV model in mice that relies on conditional expression of the core, E1, E2, and NS2 proteins and the Cre/loxP switching system [5,6]; we showed that the injection of an Ad-Cre vector enhanced the frequency of HCV-specific activated CD8 T cells in the liver of these mice and caused liver injury. However, the Ad-Cre adenovirus vector alone causes acute hepatitis in wild-type mice. Nevertheless, the transgenic model was useful for evaluating interactions between the host immune system and viral protein (serum ALT level over 2,000 IU/L) [5]; HCV core protein levels were reduced and expression of this protein was transient (about 2 weeks). Therefore, this Ad-Cre-dependent model cannot be used to effectively investigate immune responses to chronic HCV hepatitis.

Here, we used poly (I:C)-induced expression of Cre recombinase to generate HCV transgenic mice in order to study the effect of HCV protein and confirmed that these mice developed chronic active hepatitis–including steatosis, lipid deposition, and hepatocellular carcinoma. These pathological findings in the transgenic mice were very similar to those in humans with chronic hepatitis C; therefore, this mouse model of HCV may be useful for analyzing the immune response to chronic hepatitis. However, experimental results obtained with this mouse model may not directly translate to clinical findings from patients with HCV infection because the expression of HCV proteins was not liver specific in these mice. Furthermore, poly(I:C) injection can activate innate immune responses and, consequently, might induce temporary liver injury [18]. Additionally, poly(I:C) injection has an adjuvant effect; specifically, it stimulates TLR3 signaling [19].

To evaluate whether poly(I:C) injection caused hepatitis in CN2-29$^{(+/-)}$/MxCre$^{(-/-)}$ mice, we examined serum ALT levels and liver histology following poly(I:C) injection. We found that, following poly(I:C) injection, serum ALT levels in CN2-29$^{(+/-)}$/MxCre$^{(-/-)}$ mice increased, reached a peak one day after injection, declined from day 1 to day 6, and were not elevated thereafter; this time-course indicated that poly(I:C) injection alone did not induced continuous liver injury (figure S6). Based on these findings, we believe that the effects of poly(I:C) injection in these mice did not confound our analysis of chronic hepatitis.

Immunization with rVV-N25 suppressed HCV protein levels in the liver, and this suppression was associated with ameliorated pathological chronic hepatitis findings (see Figure 3). Importantly, rVV-N25 treatment did not cause liver injury based on the serum ALT levels; therefore, this treatment was unlikely to have cytopathic effects on infected hepatocytes. These findings provided strong evidence that rVV-N25 treatment effectively halted the progression of chronic hepatitis. Immunization with plasmid DNA or with recombinant vaccinia virus can effectively induce cellular and humoral immune responses and exert a protective effect against challenge with HCV infection [20,21]. However, findings from these previous studies revealed HCV immunization of both uninfected, naïve animals and immune-tolerant animals induced a HCV-specific immune response. In the model describe here; the animals were immune competent for HCV; therefore, our findings provided further important evidence that rVV-N25 was effective in the treatment of chronic hepatitis.

In addition, we demonstrated that rVV-N25 treatment in the absence of CD4 and CD8 T cells had no effect on HCV clearance. This important observation indicated that rVV-N25-induced HCV clearance was mediated by CD4 and CD8 T cells. Many studies have shown that spontaneous viral clearance during acute HCV infection is characterized by a vigorous, broadly reactive CD4 and CD8 T-cell response. [8,22] HCV clearance and hepatocellular cytotoxicity are both mediated by CD8 antigen-specific (cytotoxic T lymphocyte) CTLs [23]. Consistent with these observations, rVV-N25 treatment effectively induced the accumulation of NS2-specific CD8 T cells, which express high levels of

CD107a and IFN-γin the spleen. Notably, even with rVV-N25 immunization, the frequency of activated CD8 T cells was very low, and a minimum of 2-weeks incubation was required to distinguish the difference between rVV treatments. Even if a small population of specific CD8+ T cells played a relevant role in the reduction of core protein, it is difficult to assert that the only NS2-specific CD8+ T cells were important to this reduction. However, based on the results presented in Figure 4B, we are able to conclude that at least CD8+ and/or CD4+ T cells were important to the reduction in HCV core protein. Therefore, to elucidate the mechanism of HCV protein clearance, further investigation of not only the other T cell epitopes but also other immunocompetent cells is required.

Interestingly, rVV-N25 treatment–but not the rVV-CN2 or rVV-CN5 treatment–efficiently induced a HCV-specific activated CD8 T cells response; this difference in efficacy could have one or more possible causes. The HCV structural proteins (core, E1, and E2 proteins) in the rVV-CN construct may cause the difference; Saito et al. reported that injection with plasmid constructs encoding the core protein induced a specific CTL response in BALB/c mice [24]. Reportedly, CTL activity against core or envelope protein is completely absent from transgenic mice immunized with a plasmid encoding the HCV structural proteins, but core-specific CTL activity is present in transgenic mice that were immunized with a plasmid encoding the HCV core [21]. In contrast, when recombinant vaccinia virus expressing different regions of the HCV polyprotein were injected into BALB/c mice, only the HCV core protein markedly suppressed vaccinia-specific CTL responses [25]. Thus, the HCV core protein may have an immunomodulatory function [26]. Based on these reports and our results, we hypothesize that the causes underlying the effectiveness of rVV-N25 treatment were as follows: 1) this rVV construct included the core and envelope proteins and 2) the core protein had an immune-suppressive effect on CTL induction. Therefore, we suggest that exclusion of the core and envelope antigen as immunogen is one important factor in HCV vaccine design.

Interestingly, immunization with rVV-N25 rapidly suppressed the inflammatory response; however, immunization with either of the other rVVs did not (see Figure 6A). This result indicated that rVV-N25 may modulate inflammation via innate immunity, as well as via acquired immunity. Reportedly, Toll-like receptor (TLR)-dependent recognition pathways play a role in the recognition of poxviruses [27]. TLR2 and TLR9 have also been implicated in the recognition of the vaccinia virus [28,29]. These findings indicate that TLR on dendritic cells may modulate the immunosuppressive effect of rVV-N25 in our model of HCV infection; however, further examination of this hypothesis is required. The finding that pathological symptoms in the HCV transgenic mice were completely blocked by intravenous injection of TNF-α and IL-6 neutralizing antibodies indicated that the progression of chronic hepatitis depended on inflammatory cytokines in serum, rather than the HCV protein levels in hepatocytes. Lymphocytes, macrophages, hepatocytes, and adipocytes each produce TNF-α and IL-6 [30,31], and HCV-infected patients have elevated levels of TNF-α and IL-6 [32,33]. Both cytokines also contribute to the maintenance of hepatosteatosis in mice fed a high-fat diet [34], and production of TNF-α and IL-6 is elevated in obese mice due to the low grade inflammatory response that is caused by lipid accumulation [35]. These findings indicate that both cytokines are responsible for HCV-triggered hepatosteatosis, and anti-cytokine neutralization is a potential treatment for chronic hepatitis if antiviral therapy is not successful.

The reduction of macrophages in number might be due to the induction of apoptosis by vaccinia virus *in vitro* infection as previous reported [36]. To understand the mechanisms responsible for the reduction of the number of macrophage, we performed another experiment to confirm whether the macrophages were infected with vaccinia virus inoculation. However, based on PCR analyses; vaccinia virus DNA was not present in liver tissue that contained macrophages (Figure S7). Furthermore, apoptosis of macrophages was not detected in liver samples (Data not shown). Based on these results, it is unlikely that the reduction in the number of macrophages was due to apoptosis induced by vaccinia virus infection. Although rVV-N25 reduced the number of macrophage, precise mechanism is still unknown. Further examination to elucidate the mechanism is required.

In conclusion, our findings demonstrated that rVV-N25 is a promising candidate for an HCV vaccine therapy. Additionally, the findings of this study indicate that rVV-N25 immunization can be used for prevention of HCV infection and as an antiviral therapy against ongoing HCV infection.

Materials and Methods

Ethics Statement

All animal care and experimental procedures were performed according to the guidelines established by the Tokyo Metropolitan Institute of Medical Science Subcommittee on Laboratory Animal Care; these guidelines conform to the Fundamental Guidelines for Proper Conduct of Animal Experiment and Related Activities in Academic Research Institutions under the jurisdiction of the Ministry of Education, Culture, Sports, Science and Technology, Japan, 2006. All protocols were approved by the Committee on the Ethics of Animal Experiments of the Tokyo Metropolitan Institute of Medical Science (Permit Number: 11–078). All efforts were made to minimize the suffering of the animals.

Animals

R6CN2 HCV cDNA (nt 294–3435) [37] and full genomic HCV cDNA (nt 1–9611) [38,39] were cloned from a blood sample taken from a patient (#R6) with chronic active hepatitis (Text S1). The infectious titer of this blood sample has been previously reported [40]. R6CN2HCV and R6CN5HCV transgenic mice were bred with Mx1-Cre transgenic mice (purchased from Jackson Laboratory) to produce R6CN2HCV-MxCre and R6CN5HCV-MxCre transgenic mice, which were designated CN2-29$^{(+/-)}$/MxCre$^{(+/-)}$ and RzCN5-15$^{(+/-)}$/MxCre$^{(+/-)}$ mice, respectively. Cre expression in the livers of these mice was induced by intraperitoneal injection of polyinosinic acid–polycytidylic acid [poly(I:C)] (GE Healthcare UK Ltd., Buckinghamshire, England); 300 μL of a poly(I:C) solution (1 mg/mL in phosphate-buffered saline [PBS]) was injected three times at 48-h intervals. All animal care and experimental procedures were performed according to the guidelines established by the Tokyo Metropolitan Institute of Medical Science Subcommittee on Laboratory Animal Care.

Histology and Immunohistochemical Staining

Tissue samples were fixed in 4% paraformaldehyde in PBS, embedded in paraffin, sectioned (4-μm thickness), and stained with hematoxylin and eosin (H&E). Staining with periodic acid–Schiff stain, Azan stain, silver, or Oil-red-O was also performed to visualize glycogen degeneration, fibrillization, reticular fiber degeneration, or lipid degeneration, respectively.

For immunohistochemical staining, unfixed frozen liver sections were fixed in 4% paraformaldehyde for 10 min and then incubated with blocking buffer (1% bovine serum albumin in PBS) for 30 min at room temperature. Subsequently, the sections were incubated with biotinylated mouse anti-HCV core mono-

clonal antibody (5E3) for 2 h at room temperature. After being washed with PBS, the sections were incubated with streptavidin–Alexa Fluor 488 (Invitrogen). The nuclei were stained with 4',6-diamidino-2-phenylindole (DAPI). Fluorescence was observed using a confocal laser microscope (Laser scanning microscope 510, Carl Zeiss).

Generation of rVVs

The pBR322-based plasmid vector pBMSF7C contained the ATI/p7.5 hybrid promoter within the hemagglutinin gene region of the vaccinia virus, which was reconstructed from the pSFJ1-10 plasmid and pBM vector [41,42]. Separate full-length cDNAs encoding either the HCV structural protein, nonstructural protein, or all HCV proteins were cloned from HCV R6 strain (genotype 1b) RNA by RT-PCR. Each cDNA was inserted into a separate pBMSF7C vector downstream of the pBMSF7C ATI/p7.5 hybrid promoter; the final designation of each recombinant plasmid was pBMSF7C-CN2, pBMSF7C-N25, or pBMSF-CN5 (Figure 2). They were then transfected into primary rabbit kidney cells infected with LC16m8 (multiplicity of infection = 10). The virus–cell mixture was harvested 24 h after the initial transfection by scrapping; the mixture was then frozen at −80°C until use. The hemagglutinin-negative recombinant viruses were cloned as previously described [42] and named rVV-CN2, rVV-N25, or rVV-CN5. Insertion of the HCV protein genes into the LC16m8 genome was confirmed by direct PCR, and expression of each protein from the recombinant viruses was confirmed by western blot analysis. The titers of rVV-CN2, rVV-N25, and rVV-CN5 were determined using a standard plaque assay and RK13 cells.

Statistical Analysis

Data are shown as mean ± SD. Data were analyzed using the nonparametric Mann–Whitney or Kruskal–Wallis tests or ANOVA as appropriate; GraphPad Prism 5 for Macintosh (GraphPad) was used for all analyses. *P* values <0.05 were considered statistically significant.

Supporting Information

Figure S1 HAI score of liver samples taken from CN2-29$^{(+/-)}$/MxCre$^{(+/-)}$ mice.
(EPS)

Figure S2 Lipid degeneration in samples of liver taken from CN2-29$^{(+/-)}$/MxCre$^{(+/-)}$ mice.
(EPS)

Figure S3 HCV protein expression after infection of LC16m8, rVV-CN2, rVV-N25, or rVV-CN5 into HepG2 cells.
(EPS)

Figure S4 Effects of treatment with rVV-N25 in RzCN5-15$^{(+/-)}$/MxCre$^{(+/-)}$ mice.
(EPS)

Figure S5 Daily cytokine profiles of the serum from CN2-29$^{(+/-)}$/MxCre$^{(+/-)}$ mice during the week following inoculation with LC16m8, rVV-CN2, rVV-N25, or rVV-CN5.
(EPS)

Figure S6 The immune response following poly(I:C) injection in the acute phase.
(EPS)

Figure S7 Detection of vaccinia virus DNA in the skin, liver, and spleen after inoculation with attenuated vaccinia virus (Lister strain) or highly attenuated vaccinia virus (LC16m8 strain).
(EPS)

Table S1 Incidence of hepatocellular carcinoma in male and female transgenic mice at 360, 480, and 600 days after poly(I:C) injection.
(EPS)

Text S1 Supporting information including material and methods, and references.
(DOCX)

Acknowledgments

We thank Dr. Fukashi Murai for supporting this study. We also thank Dr. Keiji Tanaka for providing the MxCre mice, Dr. Shigeo Koyasu for providing the GK1.5 (anti-CD4) and 53–6.72 (anti-CD8) monoclonal antibodies, and Dr Takashi Tokuhisa for helpful discussions.

Author Contributions

Performed the experiments: SS KK TC Y. Tobita TO FY Y. Tokunaga. Analyzed the data: SS KK TC MK. Contributed reagents/materials/analysis tools: KT-K TW TT MM K. Mizuno YH TH K. Matsushima. Wrote the paper: SS KK MK. Study concept and design: MK.

References

1. Lauer GM, Walker BD (2001) Hepatitis C virus infection. N Engl J Med 345: 41–52.
2. Alter MJ (1995) Epidemiology of hepatitis C in the West. Semin Liver Dis 15: 5–14.
3. Kawamura T, Furusaka A, Koziel MJ, Chung RT, Wang TC, et al. (1997) Transgenic expression of hepatitis C virus structural proteins in the mouse. Hepatology 25: 1014–1021.
4. Moriya K, Fujie H, Shintani Y, Yotsuyanagi H, Tsutsumi T, et al. (1998) The core protein of hepatitis C virus induces hepatocellular carcinoma in transgenic mice. Nat Med 4: 1065–1067.
5. Wakita T, Katsume A, Kato J, Taya C, Yonekawa H, et al. (2000) Possible role of cytotoxic T cells in acute liver injury in hepatitis C virus cDNA transgenic mice mediated by Cre/loxP system. J Med Virol 62: 308–317.
6. Wakita T, Taya C, Katsume A, Kato J, Yonekawa H, et al. (1998) Efficient conditional transgene expression in hepatitis C virus cDNA transgenic mice mediated by the Cre/loxP system. J Biol Chem 273: 9001–9006.
7. Folgori A, Capone S, Ruggeri L, Meola A, Sporeno E, et al. (2006) A T-cell HCV vaccine eliciting effective immunity against heterologous virus challenge in chimpanzees. Nat Med 12: 190–197.
8. Chisari FV, Ferrari C (1995) Hepatitis B virus immunopathology. Springer Semin Immunopathol 17: 261–281.
9. Machida K, Tsukiyama-Kohara K, Seike E, Tone S, Shibasaki F, et al. (2001) Inhibition of cytochrome c release in Fas-mediated signaling pathway in transgenic mice induced to express hepatitis C viral proteins. J Biol Chem 276: 12140–12146.
10. Kuhn R, Schwenk F, Aguet M, Rajewsky K (1995) Inducible gene targeting in mice. Science 269: 1427–1429.
11. Li K, Chen Z, Kato N, Gale M Jr, Lemon SM (2005) Distinct poly(I-C) and virus-activated signaling pathways leading to interferon-beta production in hepatocytes. J Biol Chem 280: 16739–16747.
12. Sugimoto M, Yamanouchi K (1994) Characteristics of an attenuated vaccinia virus strain, LC16m0, and its recombinant virus vaccines. Vaccine 12: 675–681.
13. Youn JW, Hu YW, Tricoche N, Pfahler W, Shata MT, et al. (2008) Evidence for protection against chronic hepatitis C virus infection in chimpanzees by immunization with replicating recombinant vaccinia virus. J Virol 82: 10896–10905.
14. Guidotti LG, Rochford R, Chung J, Shapiro M, Purcell R, et al. (1999) Viral clearance without destruction of infected cells during acute HBV infection. Science 284: 825–829.
15. Burkett MW, Shafer-Weaver KA, Strobl S, Baseler M, Malyguine A (2005) A novel flow cytometric assay for evaluating cell-mediated cytotoxicity. J Immunother 28: 396–402.

16. Pasquinelli C, Shoenberger JM, Chung J, Chang KM, Guidotti LG, et al. (1997) Hepatitis C virus core and E2 protein expression in transgenic mice. Hepatology 25: 719–727.
17. Lerat H, Honda M, Beard MR, Loesch K, Sun J, et al. (2002) Steatosis and liver cancer in transgenic mice expressing the structural and nonstructural proteins of hepatitis C virus. Gastroenterology 122: 352–365.
18. Lang KS, Georgiev P, Recher M, Navarini AA, Bergthaler A, et al. (2006) Immunoprivileged status of the liver is controlled by Toll-like receptor 3 signaling. The Journal of clinical investigation 116: 2456–2463.
19. Jasani B, Navabi H, Adams M (2009) Ampligen: a potential toll-like 3 receptor adjuvant for immunotherapy of cancer. Vaccine 27: 3401–3404.
20. Elmowalid GA, Qiao M, Jeong SH, Borg BB, Baumert TF, et al. (2007) Immunization with hepatitis C virus-like particles results in control of hepatitis C virus infection in chimpanzees. Proc Natl Acad Sci U S A 104: 8427–8432.
21. Satoi J, Murata K, Lechmann M, Manickan E, Zhang Z, et al. (2001) Genetic immunization of wild-type and hepatitis C virus transgenic mice reveals a hierarchy of cellular immune response and tolerance induction against hepatitis C virus structural proteins. J Virol 75: 12121–12127.
22. Crispe IN (2009) The liver as a lymphoid organ. Annu Rev Immunol 27: 147–163.
23. Chisari FV (2005) Unscrambling hepatitis C virus-host interactions. Nature 436: 930–932.
24. Saito T, Sherman GJ, Kurokohchi K, Guo ZP, Donets M, et al. (1997) Plasmid DNA-based immunization for hepatitis C virus structural proteins: immune responses in mice. Gastroenterology 112: 1321–1330.
25. Large MK, Kittlesen DJ, Hahn YS (1999) Suppression of host immune response by the core protein of hepatitis C virus: possible implications for hepatitis C virus persistence. Journal of immunology 162: 931–938.
26. Dustin LB, Rice CM (2007) Flying under the radar: the immunobiology of hepatitis C. Annu Rev Immunol 25: 71–99.
27. Bowie A, Kiss-Toth E, Symons JA, Smith GL, Dower SK, et al. (2000) A46R and A52R from vaccinia virus are antagonists of host IL-1 and toll-like receptor signaling. Proc Natl Acad Sci U S A 97: 10162–10167.
28. Zhu J, Martinez J, Huang X, Yang Y (2007) Innate immunity against vaccinia virus is mediated by TLR2 and requires TLR-independent production of IFN-beta. Blood 109: 619–625.
29. Samuelsson C, Hausmann J, Lauterbach H, Schmidt M, Akira S, et al. (2008) Survival of lethal poxvirus infection in mice depends on TLR9, and therapeutic vaccination provides protection. J Clin Invest 118: 1776–1784.
30. Sheikh MY, Choi J, Qadri I, Friedman JE, Sanyal AJ (2008) Hepatitis C virus infection: molecular pathways to metabolic syndrome. Hepatology 47: 2127–2133.
31. Tilg H, Moschen AR, Kaser A, Pines A, Dotan I (2008) Gut, inflammation and osteoporosis: basic and clinical concepts. Gut 57: 684–694.
32. Malaguarnera M, Di Fazio I, Laurino A, Ferlito L, Romano M, et al. (1997) Serum interleukin 6 concentrations in chronic hepatitis C patients before and after interferon-alpha treatment. Int J Clin Pharmacol Ther 35: 385–388.
33. Larrea E, Garcia N, Qian C, Civeira MP, Prieto J (1996) Tumor necrosis factor alpha gene expression and the response to interferon in chronic hepatitis C. Hepatology 23: 210–217.
34. Park EJ, Lee JH, Yu GY, He G, Ali SR, et al. (2010) Dietary and genetic obesity promote liver inflammation and tumorigenesis by enhancing IL-6 and TNF expression. Cell 140: 197–208.
35. Gregor MF, Hotamisligil GS (2011) Inflammatory mechanisms in obesity. Annu Rev Immunol 29: 415–445.
36. Humlova Z, Vokurka M, Esteban M, Melkova Z (2002) Vaccinia virus induces apoptosis of infected macrophages. The Journal of general virology 83: 2821–2832.
37. Choo QL, Kuo G, Weiner AJ, Overby LR, Bradley DW, et al. (1989) Isolation of a cDNA clone derived from a blood-borne non-A, non-B viral hepatitis genome. Science 244: 359–362.
38. Tsukiyama-Kohara K, Tone S, Maruyama I, Inoue K, Katsume A, et al. (2004) Activation of the CKI-CDK-Rb-E2F pathway in full genome hepatitis C virus-expressing cells. J Biol Chem 279: 14531–14541.
39. Nishimura T, Kohara M, Izumi K, Kasama Y, Hirata Y, et al. (2009) Hepatitis C virus impairs p53 via persistent overexpression of 3beta-hydroxysterol Delta24-reductase. J Biol Chem 284: 36442–36452.
40. Shimizu YK, Purcell RH, Yoshikura H (1993) Correlation between the infectivity of hepatitis C virus in vivo and its infectivity in vitro. Proc Natl Acad Sci U S A 90: 6037–6041.
41. Yasui F, Kai C, Kitabatake M, Inoue S, Yoneda M, et al. (2008) Prior immunization with severe acute respiratory syndrome (SARS)-associated coronavirus (SARS-CoV) nucleocapsid protein causes severe pneumonia in mice infected with SARS-CoV. J Immunol 181: 6337–6348.
42. Kitabatake M, Inoue S, Yasui F, Yokochi S, Arai M, et al. (2007) SARS-CoV spike protein-expressing recombinant vaccinia virus efficiently induces neutralizing antibodies in rabbits pre-immunized with vaccinia virus. Vaccine 25: 630–637.

Arch Virol
DOI 10.1007/s00705-013-1618-6

ORIGINAL ARTICLE

Dynamics of cellular immune responses in the acute phase of dengue virus infection

Tomoyuki Yoshida · Tsutomu Omatsu · Akatsuki Saito · Yuko Katakai · Yuki Iwasaki · Terue Kurosawa · Masataka Hamano · Atsunori Higashino · Shinichiro Nakamura · Tomohiko Takasaki · Yasuhiro Yasutomi · Ichiro Kurane · Hirofumi Akari

Received: 13 June 2012 / Accepted: 12 December 2012

Abstract In this study, we examined the dynamics of cellular immune responses in the acute phase of dengue virus (DENV) infection in a marmoset model. Here, we found that DENV infection in marmosets greatly induced responses of CD4/CD8 central memory T and NKT cells. Interestingly, the strength of the immune response was greater in animals infected with a dengue fever strain than in those infected with a dengue hemorrhagic fever strain of DENV. In contrast, when animals were re-challenged with the same DENV strain used for primary infection, the neutralizing antibody induced appeared to play a critical role in sterilizing inhibition against viral replication, resulting in strong but delayed responses of CD4/CD8 central memory T and NKT cells. The results in this study may help to better understand the dynamics of cellular and humoral immune responses in the control of DENV infection.

T. Yoshida and T. Omatsu contributed equally to this study.

Electronic supplementary material The online version of this article (doi:10.1007/s00705-013-1618-6) contains supplementary material, which is available to authorized users.

T. Yoshida · Y. Iwasaki · T. Kurosawa · M. Hamano · Y. Yasutomi · H. Akari
Tsukuba Primate Research Center, National Institute of Biomedical Innovation, 1-1 Hachimandai, Tsukuba, Ibaraki 305-0843, Japan

T. Yoshida (✉) · A. Saito · A. Higashino · H. Akari (✉)
Center for Human Evolution Modeling Research, Primate Research Institute, Kyoto University, Inuyama, Aichi 484-8506, Japan
e-mail: yoshida.tomoyuki.4w@kyoto-u.ac.jp

H. Akari
e-mail: akari.hirofumi.5z@kyoto-u.ac.jp

Introduction

Dengue virus (DENV) causes the most prevalent arthropod-borne viral infections in the world [29]. Infection with one of the four serotypes of DENV can lead to dengue fever (DF) and sometimes to fatal dengue hemorrhagic fever (DHF) or dengue shock syndrome (DSS) [12]. The serious diseases are more likely to develop after secondary infection with a serotype of DENV that is different from that of the primary infection. Infection with DENV induces a high-titered neutralizing antibody response that can provide long-term immunity to the homologous DENV serotype, while the effect of the antibody on the heterologous serotypes is transient [22]. On the other hand, enhanced pathogenicity after secondary DENV infection appears to be explained by antibody-dependent enhancement (ADE). Mouse and monkey experiments have shown that subneutralizing levels of DENV-specific antibodies actually enhance infection [1, 6, 11]. Thus, the development of an effective tetravalent dengue vaccine is considered to be an important public-health priority. Recently, several DENV vaccine candidates have undergone clinical trials, and most of them target the induction of neutralizing antibodies [20].

T. Omatsu · T. Takasaki · I. Kurane
Department of Virology I, National Institute of Infectious Diseases, 1-23-1 Toyama, Shinjuku-ku, Tokyo 162-8640, Japan

Y. Katakai
Corporation for Production and Research of Laboratory Primates, 1-1 Hachimandai, Tsukuba, Ibaraki 305-0843, Japan

S. Nakamura
Research Center for Animal Life Science, Shiga University of Medical Science, Seta Tsukinowa-cho, Otsu, Shiga 520-2192, Japan

Published online: 05 February 2013

Research of the long-term immune response in humans has provided several interesting parallels to the data. It was reported that complete cross-protective immunity from heterologous challenge was induced in individuals 1–2 months after a primary DENV infection, with partial immunity present up to 9 months, resulting in a milder disease of shorter duration on reinfection, and that complete serotype-specific immunity against symptomatic dengue was observed up to 18 months postinfection [30]. Guzman and Sierra have previously recorded the long-term presence of both DENV-specific antibodies and T cells up to 20 years after natural infections [10, 31]. Of note, increased T cell activation is reportedly associated with severe dengue disease [7, 8]. Thus, the balance between humoral and cellular immunity may be important in the control of dengue diseases.

However, the details regarding the implication of humoral and cellular immunity in controlling DENV infection remain to be elucidated. Previously, passive transfer of either monoclonal or polyclonal antibodies was shown to protect against homologous DENV challenge [13, 15, 16]. It was also reported that neutralizing antibodies played a greater role than cytotoxic T lymphocyte (CTL) responses in heterologous protection against secondary DENV infection *in vivo* in IFN-α/βR$^{-/-}$ and IFNγR$^{-/-}$ mouse models [18]. Moreover, CD4$^+$ T cell depletion did not affect the DENV-specific IgG or IgM Ab titers or their neutralizing activity in the IFNγR$^{-/-}$ mouse model [36]. On the other hand, there are several reports showing that cellular immunity rather than humoral immunity plays an important role in the clearance of DENV. For example, in adoptive transfer experiments, although cross-reactive DENV-1-specific CD8$^+$ T cells did not mediate protection against a lethal DENV-2 infection, adoptive transfer of CD4$^+$ T cells alone mediated protection and delayed mortality in IFN-α/βR$^{-/-}$ and IFNγR$^{-/-}$ mouse models [39]. It has also been demonstrated that CD8$^+$ T lymphocytes have a direct role in protection against DENV challenge in the IFN-α/βR$^{-/-}$ mouse model of DENV infection by depleting CD8$^+$ T cells [35]. In addition, previous data from adoptive-transfer experiments in BALB/c mice showed that cross-reactive memory CD8$^+$ T cells were preferentially activated by the secondary DENV infection, resulting in augmented IFN-γ and tumor necrosis factor-α (TNF-α) responses, and this effect was serotype-dependent [2, 3]. Although it has previously been suggested that inducing neutralizing antibodies against DENV may play an important role in controlling DENV infection, CTLs are also proposed to contribute to clearance during primary DENV infection and to pathogenesis during secondary heterologous infection in the BALB/c mouse model [4].

Why did the mouse models of DENV infection show inconsistent results *in vivo*? One of the reasons could be that these results were obtained mainly from genetically manipulated mice such as IFN-α/βR$^{-/-}$ and IFNγR$^{-/-}$ mice. Moreover, these mice were inoculated with 10^9–10^{10} genome equivalents (GE) of DENV [27, 35, 36], which were likely in large excess compared with the 10^4-10^5 GE of DENV injected into humans by a mosquito [19]. In addition, the efficiency of DENV replication in wild mice *in vivo* is very low compared to that in humans [35].

Recently, novel non-human primate models of DENV infection using rhesus macaques as well as marmosets and tamarins have been developed [24–26, 38]. An intravenous challenge of rhesus macaques with a high dose of virus inoculum (1×10^7 GE) of DENV-2 resulted in readily visible hemorrhaging, which is one of the cardinal symptoms of human DHF [26]. It was also shown that the cellular immune response was activated due to expression of IFN-γ, TNF-α, and macrophage inflammatory protein-1 β in CD4$^+$ and CD8$^+$ T cells during primary DENV infection in rhesus macaques [20]. On the other hand, in the marmoset model of DENV infection, we observed high levels of viremia (10^5–10^7 GE/ml) after subcutaneous inoculation with 10^4–10^5 plaque-forming units (PFU) of DENV-2. Moreover, we demonstrated that DENV-specific IgM and IgG were consistently detected and that the DENV-2 genome was not detected in any of these marmosets inoculated with the same DENV-2 strain used in the primary infection [24]. It is notable that while neutralizing antibody titers were at levels of 1:20-1:80 before the re-challenge inoculation, the titers increased up to 1:160-1:640 after the re-challenge inoculation [24]. These results suggested that the secondary infection with DENV-2 induced a protective humoral immunity to DENV-2 and that DENV-infected marmoset models may be useful in order to analyze the relationship between DENV replication and the dynamics of adaptive immune responses *in vivo*.

Taking these findings into consideration, we investigated the dynamics of cellular immunity in response to primary and secondary DENV infection in the marmoset model.

Materials and methods

Animals

All animal studies were conducted in accordance with protocols of experimental procedures that were approved by the Animal Welfare and Animal Care Committee of the National Institute of Infectious Diseases, Japan, and the National Institute of Biomedical Innovation, Japan. A total of six male marmosets, weighing 258–512 g, were used. Common marmosets were purchased from Clea Japan Inc.

(Tokyo, Japan) and caged singly at 27 ± 2 °C in 50 ± 10 % humidity with a 12-h light-dark cycle (lighting from 7:00 to 19:00) at Tsukuba Primate Research Center, National Institute of Biomedical Innovation, Tsukuba, Japan. Animals were fed twice a day with a standard marmoset diet (CMS-1M, CLEA Japan) supplemented with fruit, eggs and milk. Water was given ad libitum. The animals were in healthy condition and confirmed to be negative for anti-dengue-virus antibodies before inoculation with dengue virus [24].

Cells

Cell culture was performed as described previously [24]. Vero cells were cultured in minimum essential medium (MEM, Sigma) with 10 % heat-inactivated fetal bovine serum (FBS, GIBCO) and 1 % non-essential amino acid (NEAA, Sigma) at 37 °C in 5 % CO_2. C6/36 cells were cultured in MEM with 10 % FBS and 1 % NEAA at 28 °C in 5 % CO_2.

Virus

DENV type 2 (DENV-2) strain DHF0663 (accession no. AB189122) and strain D2/Hu/Maldives/77/2008NIID (Mal/77/08) were used for inoculation studies. The DENV-2, DHF0663 strain was isolated from a DHF case in Indonesia. The DENV-2 Mal/77/08 strain was isolated from imported DF cases from the Maldives. For all DENV strains, isolated clinical samples were propagated in C6/36 cells and were used within four passages on C6/36 cells. Culture supernatant from infected C6/36 cells was

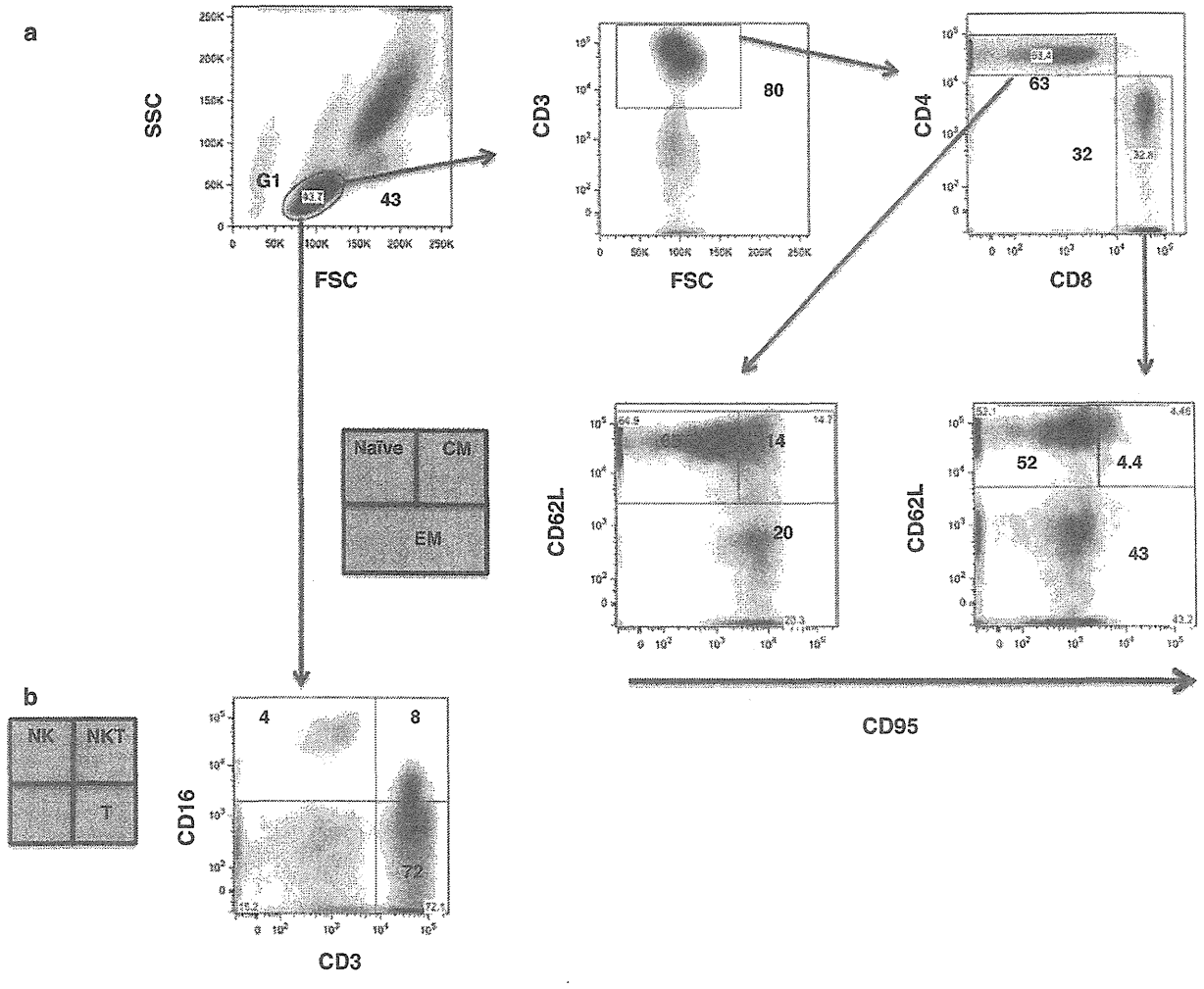

Fig. 1 Flow cytometric analysis of naïve, central/effector memory T cells and NK/NKT cells in marmosets. (a) Gating strategy to indentify CD4 and CD8 T, NK and NKT cells. The G1 population was selected and analyzed for CD4 and CD8 T, NK and NKT cells. (a) Profiling of naïve, central memory, and effector memory CD4 and CD8 T cells in total CD4 and CD8 T cells. (b) Profiling of NK and NKT cells in total lymphocytes. Results shown are representative of three healthy marmosets used in this study

centrifuged at 3,000 rpm for 5 min to remove cell debris and then stored at −80 °C until use.

Infection of the marmosets with DENV

In the challenge experiments, profiling of the key adaptive and innate immune cells in the marmosets after infection with DENV-2 was done. For primary DENV infection, four marmosets were inoculated subcutaneously in the back with either 1.9×10^5 PFU of the DENV-2 Mal/77/08 strain (Cj08-007, Cj07-011) or 1.8×10^4 PFU of the DHF0663 strain (Cj07-006, Cj07-008) [24]. In the case of the DENV re-challenge experiment, two marmosets initially inoculated with 1.8×10^5 PFU of the DHF0663 strain were re-inoculated 33 weeks after the primary challenge with 1.8×10^5 PFU of the same strain (Cj07-007, Cj07-014) [24]. Blood samples were collected on days 0, 1, 3, 7, 14, and 21 after inoculation and were used for virus titration and flow cytometric analysis. Inoculation with DENV and blood drawing were performed under anesthesia with 5 mg/kg of ketamine hydrochloride. Day 0 was defined as the day of virus inoculation. The viral loads in marmosets obtained in a previous study are shown in Supplementary Figure 1 [24].

Flow cytometry

Flow cytometry was performed as described previously [37]. Fifty microliters of whole blood from marmosets was stained with combinations of fluorescence-conjugated monoclonal antibodies; anti-CD3 (SP34-2; Becton Dickinson), anti-CD4 (L200; BD Pharmingen), anti-CD8 (CLB-T8/4H8; Sanquin), anti-CD16 (3G8; BD Pharmingen), anti-CD95 (DX2; BD Pharmingen), and anti-CD62L (145/15; Miltenyi Biotec). Then, erythrocytes were lysed with FACS lysing solution (Becton Dickinson). After washing with a sample buffer containing phosphate-buffered saline (PBS) and 1 % FBS, the labeled cells were resuspended in a fix buffer containing PBS and 1 % formaldehyde. The expression of these markers on the lymphocytes was analyzed using a FACSCanto II flow cytometer (Becton Dickinson). The data analysis was conducted using FlowJo software (Treestar, Inc.). Results are shown as mean ± standard deviation (SD) for the marmosets used in this study.

Table 1 Subpopulation ratios of lymphocytes in marmosets

Subpopulation name	Subpopulation ratios (Mean ± SD: %)
$CD3^+$	75.7 ± 6.4
$CD3^+CD4^+$	65.4 ± 6.8
$CD3^+CD4^+CD62L^+CD95^-$ (CD4 T_N)	65.9 ± 3.7
$CD3^+CD4^+CD62L^+CD95^+$(CD4 T_{CM})	16.4 ± 2.9
$CD3^+CD4^+CD62LCD95^{\pm}$ (CD4 T_{EM})	19.5 ± 2.5
$CD3^+CD8^+$	29.0 ± 8.0
$CD3^+CD8^+CD62L^+CD95^-$ (CD8 T_N)	66.7 ± 10.2
$CD3^+CD8^+CD62L^+CD95^+$(CD8 T_{CM})	4.7 ± 3.6
$CD3^+CD8^+CD62LCD95^{\pm}$ (CD8 T_{EM})	28.8 ± 14.8
CD3CD16 + (NK)	4.2 ± 2.6
$CD3^+CD16^+$ (NKT)	5.1 ± 3.4

SD: Standard deviation

Results shown are mean ± SD from 3 healthy marmosets

Results

Naïve central/effector memory T cells and NK/NKT cells in marmosets

Basic information regarding CD4/CD8 naïve and central/effector memory T cells and NK/NKT cells in common marmosets was unavailable. Thus, we examined the immunophenotypes of lymphocyte subsets in the marmosets (Fig. 1). The gating strategy for profiling the CD4 and CD8 T cells in the marmosets by FACS is shown in Fig. 1a. Human T cells are classically divided into three functional subsets based on their cell-surface expression of CD62L and CD95, i.e., $CD62L^+CD95^-$ naive T cells (T_N), $CD62L^+CD95^+$ central memory T cells (T_{CM}), and $CD62L^-CD95^{\pm}$ effector memory T cells (T_{EM}) [9, 21, 28]. In this study, $CD4^+$ and $CD8^+$ T_N, T_{CM}, and T_{EM} subpopulations were defined as $CD62L^+CD95^-$, $CD62L^+CD95^+$, and $CD62L^-CD95^{\pm}$, respectively (Fig. 1a and Table 1). The average ratio of $CD3^+$ T lymphocytes in the total lymphocytes of three marmosets was found to be 75.7 ± 6.4 %. The average ratio of $CD4^+$ T cells in the $CD3^+$ subset was 65.4 ± 6.8 %. The average ratios of $CD4^+$ T_N, T_{CM}, and T_{EM} cells were 65.9 ± 3.7 %, 16.4 ± 2.9 %, 19.5 ± 2.5 %, respectively. The average ratio of $CD8^+$ T cells in the $CD3^+$ subset was 29.0 ± 8.0 %. The average ratios of $CD8^+$ T_N, T_{CM}, and T_{EM} cells were 66.7 ± 10.2 %, 4.7 ± 3.6 %, 28.8 ± 14.8 %, respectively.

We recently characterized a $CD16^+$ major NK cell subset in tamarins and compared NK activity in tamarins with or without DENV infection [37, 38]. In terms of NKT cells, NK1.1 (CD161) and CD1d are generally used as markers of NKT cells [32]. However, these anti-human NK1.1 and CD1d antibodies are unlikely to cross-react with the NKT cells of the marmosets. Thus, we defined NKT cells as a population expressing both CD3 and CD16 as reported previously [14, 17]. The NK and NKT cell subsets were determined to be $CD3^-CD16^+$ and $CD3^+CD16^+$ lymphocytes in the marmosets. The average ratios of NK and NKT cell subsets in the lymphocytes were 4.2 ± 2.6 % and 5.1 ± 3.4 %, respectively (Table 1). We observed that the proportions of the major lymphocyte

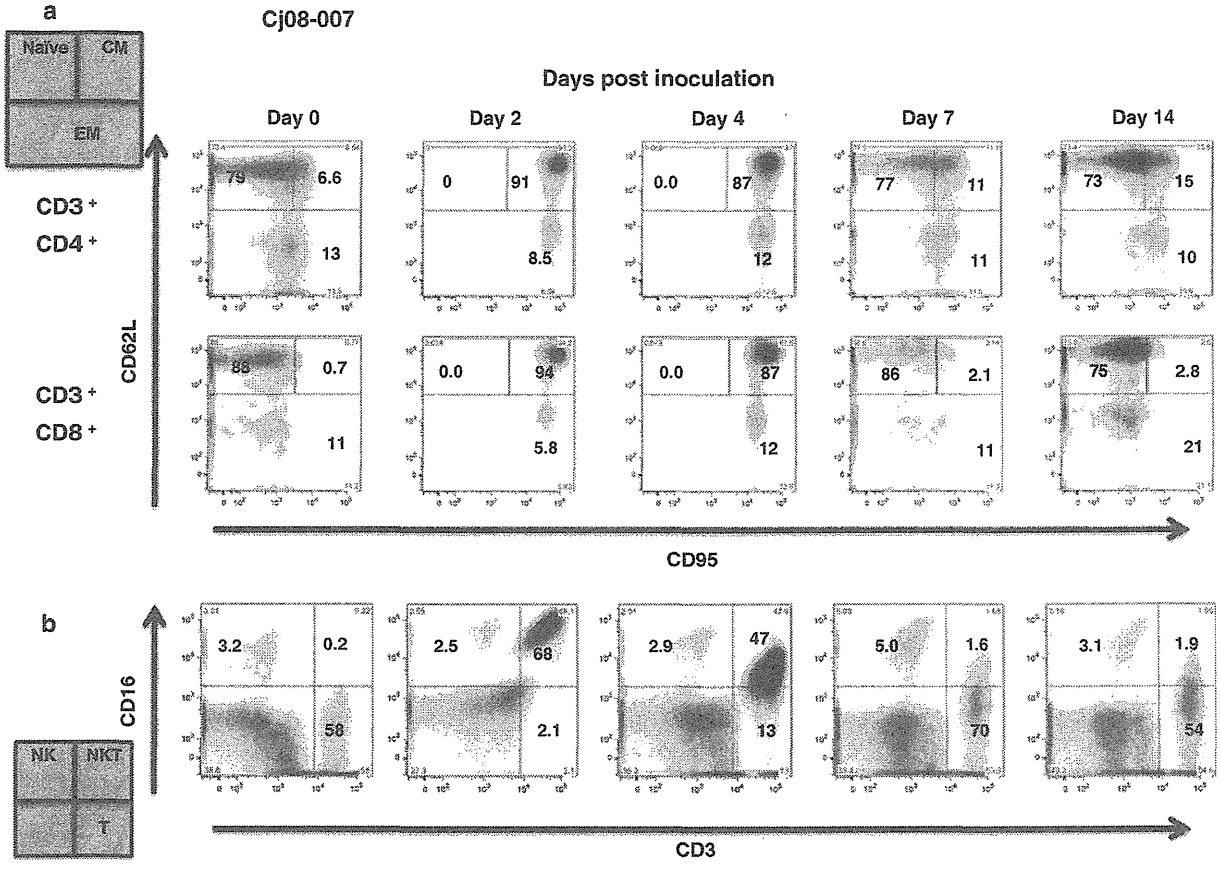

Fig. 2 Profiling of CD4 and CD8 T, NK and NKT cells in marmosets with primary infection with the DENV-2 Mal/77/08 strain. For primary DENV infection, two marmosets were inoculated subcutaneously in the back with 1.9×10^5 PFU of the DENV-2 Mal/77/08 strain. (**a**) Profiling of naïve, central memory, and effector memory CD4 and CD8 T cells in total CD4 and CD8 T cells. (**b**) Profiling of NK and NKT cells in total lymphocytes. (**a-b**) Cj08-007

subsets in the marmosets were similar to those in cynomolgus monkeys and tamarins [37, 38].

Profiling of CD4 and CD8 T, NK and NKT cells in marmosets after primary infection with DENV-2 (Mal/77/08 strain)

We investigated the cellular immune responses against DENV-2 DF strain (Mal/77/08) in marmosets. Dengue vRNA was detected in plasma samples from two marmosets on day 2 postinfection (Supplementary Fig. 1a). For the two marmosets (Cj08-007, Cj07-011), the plasma levels of vRNA reached their peaks at 9.6×10^6 and 7.0×10^6 GE/ml, respectively, on day 4 postinfection. Plasma vRNA was detected in both marmosets on days 2, 4, and 7. We then examined the profiles and frequencies of the CD4 and CD8 T, NK and NKT cells in the infected marmosets (Figs. 2–3 and Table 2). $CD4^+$ T_{CM} cells drastically increased to 88.7 ± 2.8 % from 13 ± 0.4 % between day 0 and day 2 post-inoculation (Table 2). Reciprocally, $CD4^+$ T_N cells decreased to 1.6 ± 3.3 % from 74.1 ± 0.9 % at the same time. $CD4^+$ T_{EM} cells maintained the initial levels throughout the observation period. $CD8^+$ T_{CM} cells increased to 91.9 ± 5.5 % from 2.1 ± 0.8 % between day 0 day 2 post-inoculation, and reciprocally, $CD8^+$ T_N cells decreased to 2.5 ± 4.7 % from 89.9 ± 2.5 % at the same time. In addition, NK cells maintained their initial levels throughout the observation period. However, NKT cells drastically increased to 52.6 ± 17 % from 0.2 ± 0.0 % between day 0 and day 2 post-inoculation. These results suggest that CD4/CD8 T and NKT cells may efficiently respond to the Mal/77/08 strain of DENV.

Profiling of CD4 and CD8 T, NK and NKT cells in the marmosets after primary infection with DENV-2 (DHF0663 strain)

Next, we investigated cellular immune responses against another DENV-2 DHF strain (DHF0663) in marmosets.

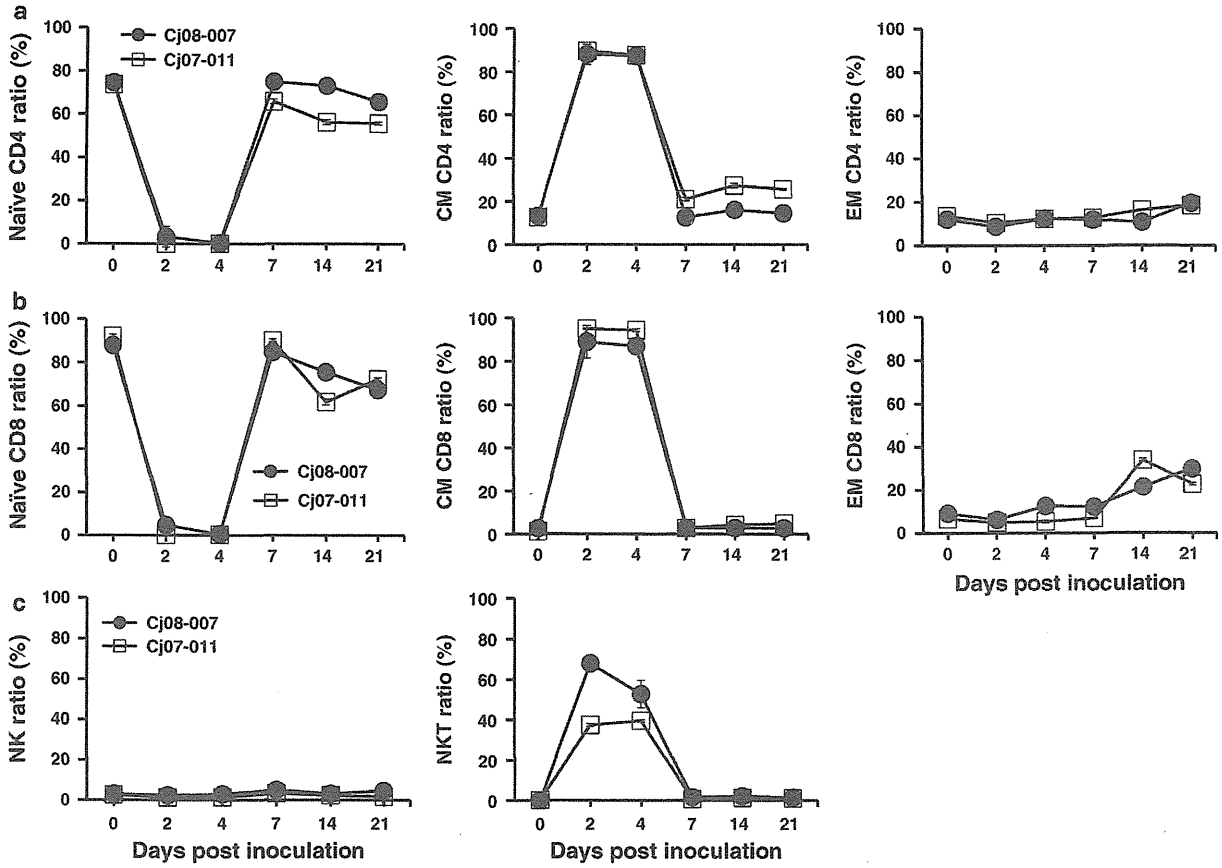

Fig. 3 Frequency of CD4 and CD8 T, NK and NKT cells in marmosets with primary infection with the DENV-2 Mal/77/08 strain. For primary DENV infection, two marmosets were inoculated subcutaneously in the back with 1.9×10^5 PFU of the DENV-2 Mal/77/08 strain. (**a**) Ratios of naïve, central memory, and effector memory CD4 T cells in total CD4 T cells. (**b**) Ratios of naïve, central memory, and effector memory CD8 T cells in total CD8 T cells. (**c**) Ratios of NK and NKT cells in total lymphocytes. (**a-c**) Cj08-007, Cj07-011

Table 2 Subpopulation ratios of lymphocytes in marmosets during primary DENV infection (Mal/77/08)

Subpopulation name		Subpopulation ratio (Mean ± SD: %)					
		Days after inoculation					
		Day 0	Day 2	Day 4	Day 7	Day 14	Day 21
$CD3^+CD4^+CD62L^+CD95''$	($CD4\ T_N$)	74.1 ± 0.9	1.6 ± 3.3	0.2 ± 0.3	70.5 ± 5.5	64.8 ± 9.7	60.8 ± 5.9
$CD3^+CD4^+CD62L^+CD95^+$	($CD4\ T_{CM}$)	13 ± 0.4	88.7 ± 2.8	87.4 ± 0.2	16.8 ± 5.0	21.6 ± 6.5	20 ± 6.4
$CD3^+CD4^+CD62LCD95^±$	($CD4\ T_{EN}$)	12.8 ± 0.9	9.5 ± 1.0	12.3 ± 0.4	12.3 ± 0.5	134 ± 3.2	189 ± 1.4
$CD3^+CD8^+CD62L^+CD95^-$	($CD8\ T_N$)	89.9 ± 2.5	2.5 ± 4.7	0.3 ± 0.3	87.5 ± 3.3	68.7 ± 79	69.8 ± 3.1
$CD3^+CD8^+CD62L^+CD95^+$	($CD8\ T_{CM}$)	2.1 ± 0.8	91.9 ± 5.5	90.6 ± 4.2	2.8 ± 0.5	3.5 ± 08	3.8 ± 1.2
$CD3^+CD8^+CD62LCD95^±$	($CD8\ T_{EN}$)	7.8 ± 1.6	5.6 ± 0.8	9.0 ± 4.1	9.5 ± 3.1	27.6 ± 72	26.3 ± 4.3
$CD3^-CD16+$	(NK)	2.9 ± 0.2	1.8 ± 0.6	2.2 ± 0.9	4.2 ± 0.9	2.8 ± 04	3.2 ± 1.7
$CD3^+CD16^+$	(NKT)	0.2 ± 0.0	52.6 ± 17	46.1 ± 8.5	1.1 ± 05	1.7 ± 05	1.2 ± 0.2

SD: Standard deviation

Results shown are mean ± SD from two marmosets as shown in Figure 3

Dengue vRNA was detected in plasma samples from the marmosets on day 2 post-infection ([24], Supplementary Fig. 1b). For the two marmosets (Cj07-006, Cj07-008), the plasma vRNA levels were found to be 3.4×10^5 and 3.8×10^5 GE/ml on day 2 and 2.0×10^6 and 9.4×10^5 GE/ml, respectively, at the peak on day 4 post-infection and became undetectable by day 14. Thus, we examined the profiles and frequencies of the $CD4^+$ and $CD8^+$ T, NK and NKT cells in these DENV-infected marmosets (Fig. 4–5 and Table 3). It was found that on day 7 post-inoculation, $CD4^+$ and $CD8^+$ T_N cells decreased, and in contrast, the T_{CM} populations increased in both marmosets; however, the changes in proportion were much less pronounced than in the case of the marmosets infected with the DF strain. We observed no consistent tendency in the kinetics of $CD4^+$ and $CD8^+$ T_{EM} cells nor in NK and NKT cells. These results suggest that the strength of T cell responses may be dependent on the strain of DENV.

Profiling of CD4 and CD8 T, NK and NKT cells in marmosets re-challenged with a DENV-2 strain

In order to examine the cellular immune responses against re-challenge with a DENV-2 DHF strain in the marmoset model, marmosets were infected twice with the same DENV-2 strain (DHF0663) with an interval of 33 weeks after the primary infection. The results showed that vRNA and NS1 antigens were not detected in plasma and that the neutralizing antibody titer was obviously increased after the secondary infection. The data indicated that the primary infection induced protective immunity, including a neutralizing antibody response to re-challenge with the same DENV strain ([24]; Supplementary Fig. 1c). We also investigated the profiles of the CD4 and CD8 T, NK and NKT cells in the marmosets (Cj07-007, Cj07-014) that were re-challenged with the same DENV-2 strain (DHF0663) (Figs. 6–7). $CD4^+$ T_{CM} cells drastically increased on day 14 post-inoculation. On the other hand,

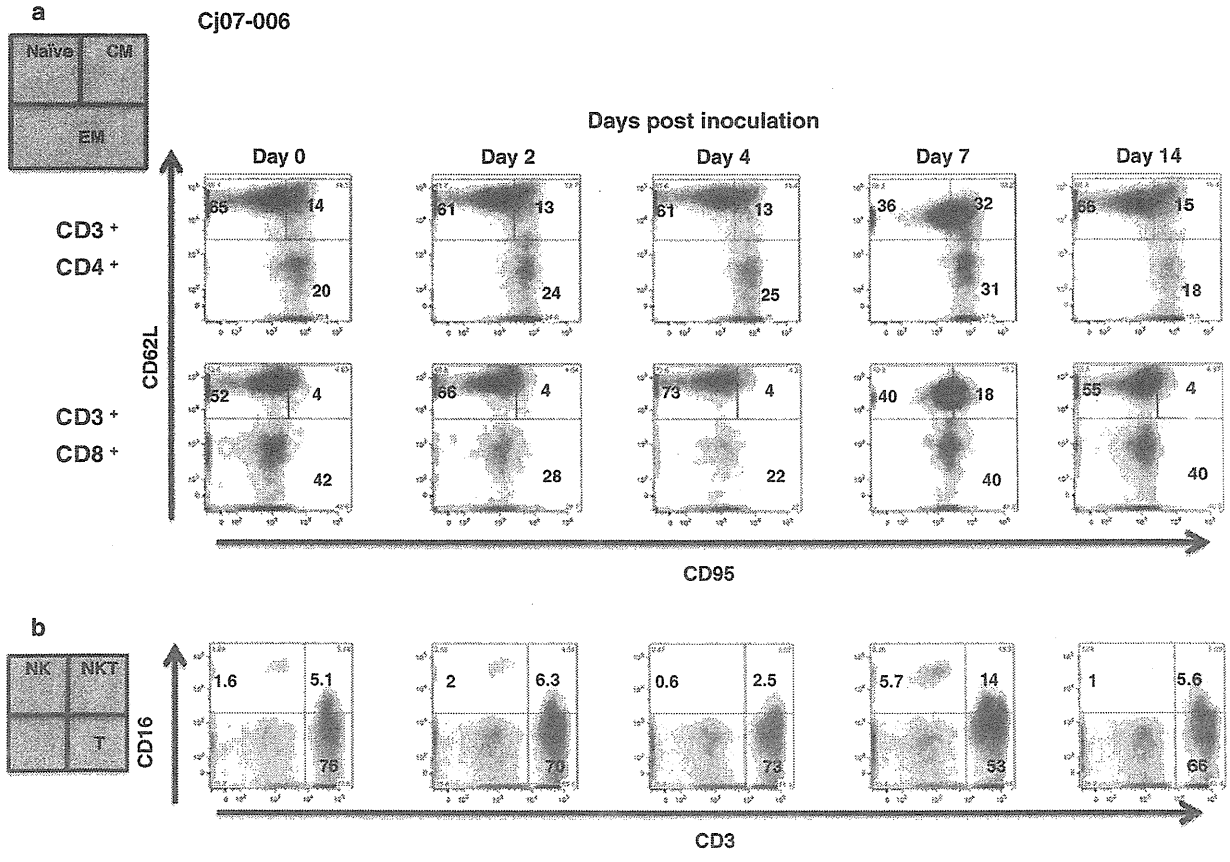

Fig. 4 Profiling of CD4 and CD8 T, NK and NKT cells in marmosets with primary infection with the DENV-2 DHF0663 strain. For primary DENV infection, two marmosets were inoculated subcutaneously in the back with 1.8×10^4 PFU of the DENV-2 DHF0663 strain. (**a**) Profiling of naïve, central memory, and effector memory CD4 and CD8 T cells in total CD4 and CD8 T cells. (**b**) Profiling of NK and NKT cells in total lymphocytes. (**a-b**) Cj07-006

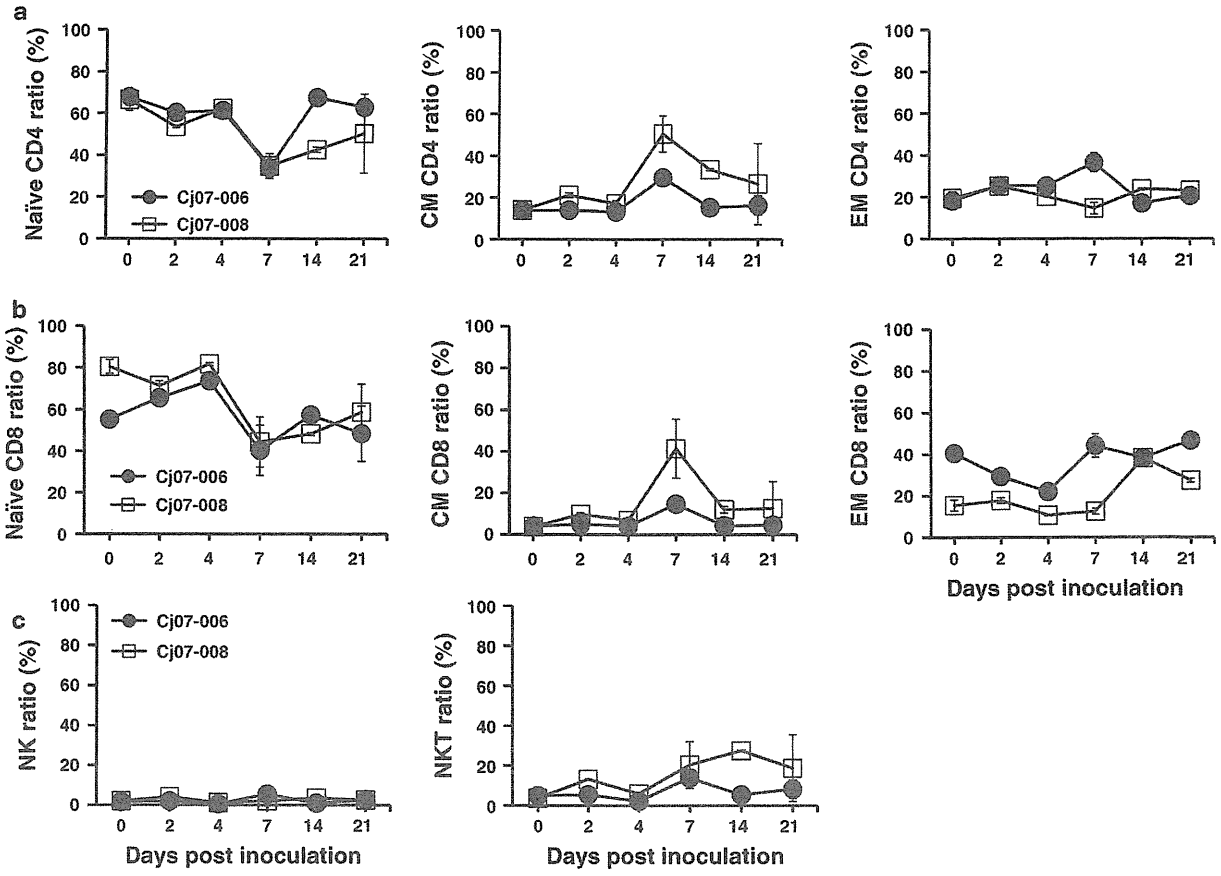

Fig. 5 Frequency of CD4 and CD8 T, NK and NKT cells in marmosets with primary infection with the DENV-2 DHF0663 strain. For primary DENV infection, two marmosets were inoculated subcutaneously in the back with 1.8×10^4 PFU of the DENV-2 DHF0663 strain. (**a**) Ratios of naïve, central memory, and effector memory CD4 T cells in total CD4 T cells. (**b**) Ratios of naïve, central memory, and effector memory CD8 T cells in total CD8 T cells. (**c**) Ratios of NK and NKT cells in total lymphocytes. (**a-c**) Cj07-006, Cj07-008

Table 3 Subpopulation ratios of lymphocytes in marmosets during primary DENV infection (DHF0663)

Subpopulation name		Subpopulation ratios (Mean ± SD: %)					
		Days after inoculation					
		Day 0	Day 2	Day 4	Day 7	Day1 4	Day 21
$CD3^+CD4^+CD62L^+CD95^-$	($CD4\ T_N$)	67.3 ± 3.6	57.0 ± 4.0	61.9 ± 0.9	34.4 ± 3.6	55.2 ± 14	56.7 ± 13
$CD3^+CD4^+CD62L^+CD95^+$	($CD4T_{CM}$)	13.9 ± 1.3	17.5 ± 4.1	15.2 ± 2.5	40.0 ± 13	33.8 ± 10	21.3 ± 12
$CD3^+CD8^+CD62L^-CD95^\pm$	($CD4\ T_{EM}$)	18.8 ± 2.2	25.3 ± 0.9	22.8 ± 2.9	25.6 ± 13	20.3 ± 4.0	21.8 ± 1.5
$CD3^+CD8^+CD62L^+CD95^-$	($CDS\ T_N$)	67.8 ± 14	68.4 ± 3.7	77.7 ± 4.6	42.2 ± 7.4	52.7 ± 5.5	53.5 ± 9.8
$CD3^+CD8^+CD62L^+CD95^-$	($CDS\ T_{CM}$)	3.9 ± 0.6	7.4 ± 2.8	5.5 ± 1.6	28 ± 17	8.1 ± 4.6	8.6 ± 8.9
$CD3^+CD8^+CD62L^-CD95^\pm$	($CDS\ T_{EM}$)	28 ± 14	23.5 ± 6.7	16.4 ± 6.5	28.3 ± 18	38.2 ± 1.9	37.0 ± 11
$CD3^-CD16^+$	(NK)	4.7 ± 1.0	4.2 ± 1.9	2.0 ± 1.1	6.3 ± 2.3	5.1 ± 2.2	7.3 ± 1.2
$CD3^+CD16^+$	(NKT)	7.8 ± 1.0	9.3 ± 4.5	5.9 ± 2.6	22.6 ± 8.4	20.6 ± 10	17.3 ± 10

SD: Standard deviation

Results shown are mean ± SD from 2 marmosets as shown in Figure 5

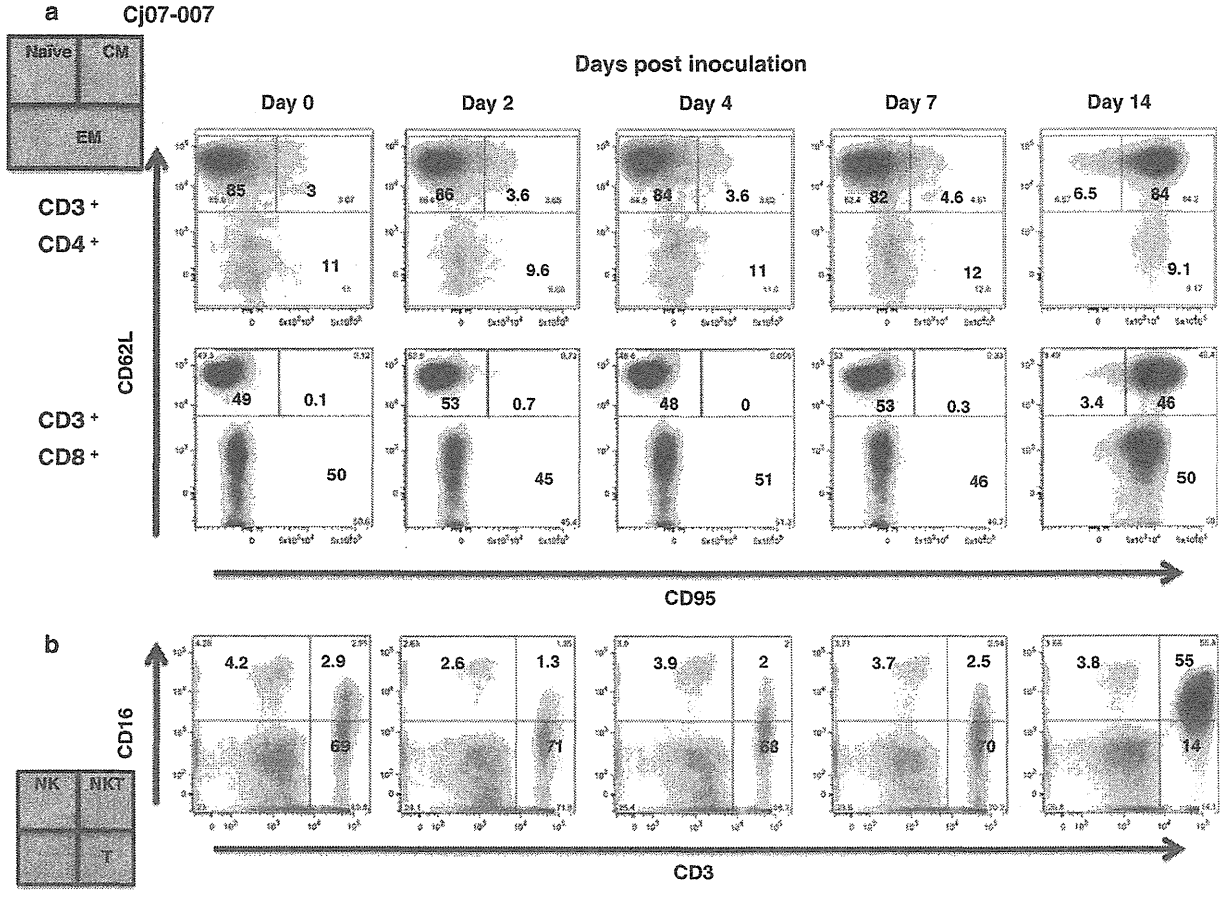

Fig. 6 Profiling of CD4 and CD8 T, NK and NKT cells in marmosets after re-challenge with the DENV-2 DHF0663 strain. Two marmosets that were initially inoculated with 1.8×10^5 PFU of the DHF0663 strain were re-inoculated 33 weeks after the primary challenge with 1.8×10^5 PFU of the same strain. (**a**) Profiling of naïve, central memory, and effector memory CD4 and CD8 T cells in total CD4 and CD8 T cells. (**b**) Profiling of NK and NKT cells in total lymphocytes. (**a-b**) Cj07-007

$CD4^+$ T_N cells decreased strongly at the same time. $CD4^+$ T_{EM} cells maintained their initial levels through the observation period. Similarly, $CD8^+$ T_{CM} and NKT cells clearly increased on day 14 post-inoculation. Importantly, these T cell responses were induced one week after the obvious induction of the neutralizing antibody in the marmosets [24]. These results suggest that the neutralizing antibody may play a critical role in the complete inhibition of the secondary DENV infection.

Discussion

In this study, we demonstrated the dynamics of the central/effector memory T cells and NK/NKT subsets against DENV infection in our marmoset model. First, we characterized the central/effector memory T and NK/NKT subsets in marmosets (Fig. 1). Second, we found that CD4/CD8 central memory T cells and NKT cells had significant responses in the primary DENV infection, and the levels appeared to be dependent on the strain of the virus employed for challenge experiments (Figs. 2–5). Finally, we found delayed responses of CD4/CD8 central memory T cells in the monkeys re-challenged with the same DENV DHF strain, despite the complete inhibition of DENV replication (Figs. 6–7).

The present study shed light on the dynamics of cellular and humoral immune responses against DENV *in vivo* in the marmoset model. Our results showed that cellular immune responses were induced earlier than antibody responses in the primary infection. Thus, our results suggest the possibility that cellular immunity may contribute, at least in part, to the control of primary DENV infection. On the other hand, in the presence of neutralizing antibodies in the re-challenged monkeys [24], delayed (on day 14 after the re-challenge) responses of CD4/CD8 central memory T cells were observed despite the complete inhibition of DENV replication. These results indicate that

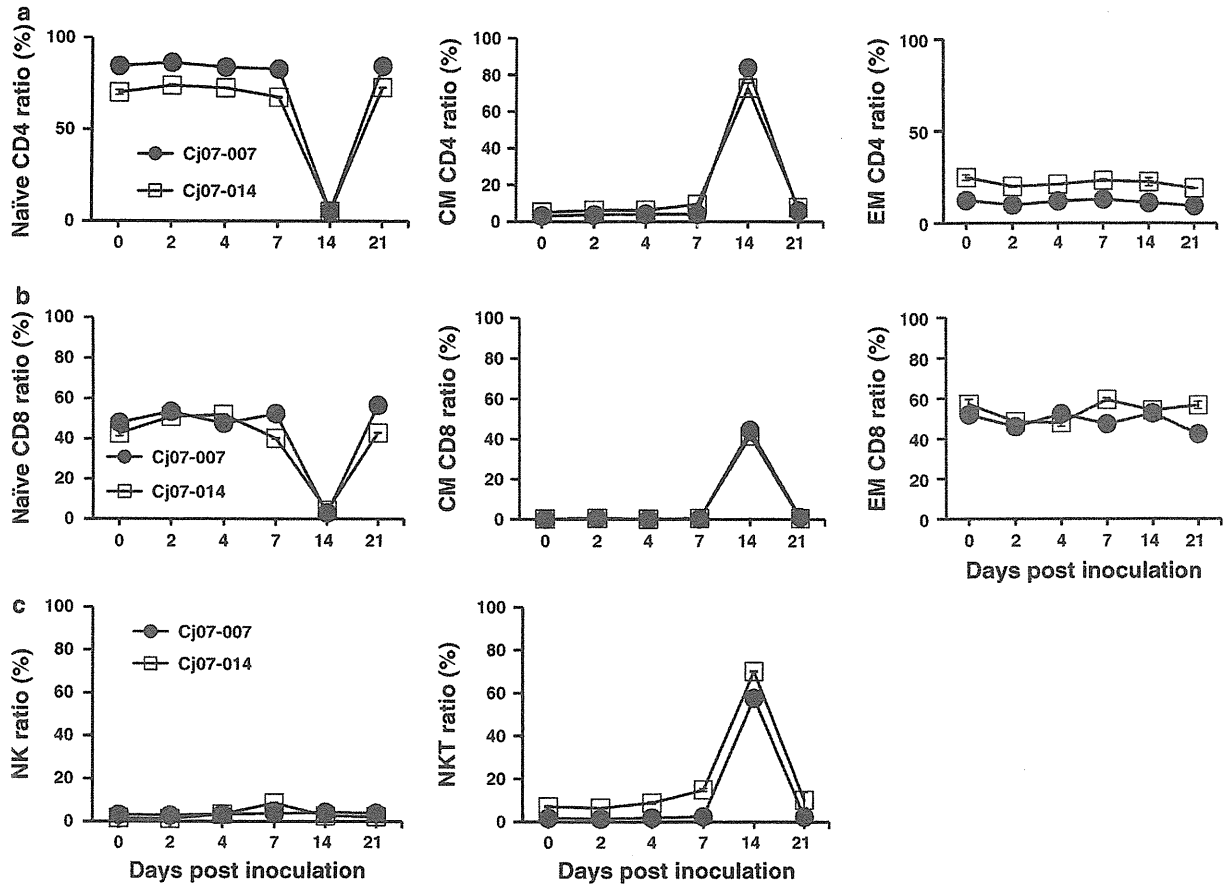

Fig. 7 Frequency of CD4 and CD8 T, NK and NKT cells in marmosets after re-challenge with the DENV-2 DHF0663 strain. Two marmosets initially inoculated with 1.8×10^5 PFU of the DHF0663 strain were re-inoculated 33 weeks after the primary challenge with 1.8×10^5 PFU of the same strain. (**a**) Ratios of naïve, central memory, and effector memory CD4 T cells in total CD4 T cells. (**b**) Ratios of naïve, central memory, and effector memory CD8 T cells in total CD8 T cells. (**c**) Ratios of NK and NKT cells in total lymphocytes. (**a-c**) Cj07-007, Cj07-014

cellular immunity is unlikely to play a major role in the control of DENV re-infection. Alternatively, it is still possible that components of cellular immunity, such as memory T cells, could partially play a helper role for the enhanced induction of neutralizing antibodies even without an apparent increase in the proportion of T_{CM}, resulting in efficient prevention of DENV replication.

It is possible that the DENV strains used in this study influence the strength of cellular immune responses. The differences in cellular immune responses between the monkeys infected with the DF and DHF strains are probably not caused by individual differences in the marmosets, because the FACS results were consistent with each pair of marmosets. It was shown previously that there was a reduction in CD3, CD4, and CD8 cells in DHF and that lower levels of CD3, CD4, and CD8 cells discriminated DHF from DF patients during the febrile stage of illness [5]. There was a significant increase in an early activation marker on $CD8^+$ T cells in children with DHF compared with DF during the febrile period of illness [8]. Another group reported that levels of peripheral blood mononuclear cell apoptosis were higher in children developing DHF [23]. Moreover, cDNA array and ELISA screening demonstrated that IFN-inducible genes, IFN-induced genes and IFN production were strongly up-regulated in DF patients when compared to DHF patients, suggesting a significant role of the IFN system during infection with DF strains when compared to DHF strains [34]. Thus, it is reasonable to assume that DHF strains might have the ability to negatively regulate T cell responses. A recent report demonstrating that the sequence of a DHF strain differed from that of a DF strain at six unique amino acid residues located in the membrane, envelope and non-structural genes [33], which supports our notion.

Alternatively, another possibility is that the strength of T cell responses might depend on the viral load. In fact, in

our results, the stronger T cell responses in monkeys infected with the DF strain were paralleled by higher viral loads, which was in contrast to the result obtained with DHF-strain-infected animals with lower viral loads. Of note, the tenfold higher challenge dose of the DF strain used in this study (1.9×10^5 PFU) compared to the DHF strain (1.8×10^4 PFU) could have simply led to tenfold higher peak viral RNA levels in monkeys infected with the DF strain. In either case, the relationship between the strength of the antiviral immune response and the viral strain remains to be elucidated. Further *in vivo* characterization of the antiviral immunity and the viral replication kinetics induced by infection with various DENV strains isolated from DF and DHF patients will help to understand the mechanism of differential disease progression in the course of DENV infection.

We observed that dengue vRNA was not detected in plasma samples from marmosets re-infected with the same DENV-2 DHF strain 33 weeks after the primary infection. This result suggests that memory B cells induced in the primary DENV infection were predominantly activated to produce neutralizing antibodies against the same DHF strain in the secondary infection in the absence of apparent cellular immune responses. A previous report showed that DENV infection induces a high-titered neutralizing antibody that can provide long-term immunity to the homologous DENV serotype [22], which is consistent with our results. By contrast, the role of cellular immune responses in the control of DENV infection remains to be elucidated. Our results in this study may suggest that cellular immune responses and neutralizing antibodies acted cooperatively to control primary DENV infection. In DENV-infected patients, it may be difficult to distinguish whether each case is primary or secondary DENV infection and also to serially collect blood samples for immunological study in the course of the infection, which is likely to be the reason for the discrepancy regarding the importance of cellular immunity in DENV infection. From this point of view, our marmoset model of DENV infection will further provide important information regarding the role of cellular immune responses in DENV infection.

Acknowledgments We would like to give special thanks to members of The Corporation for Production and Research of Laboratory Primates for technical assistance. We also appreciate Ms. Tomoko Ikoma and Mizuho Fujita for technical assistance. This work was supported by grants from the Ministry of Health, Labor and Welfare of Japan, and by the Environment Research and Technology Development Fund (D-1007) from the Ministry of the Environment of Japan.

Conflict of interest The authors declare that the research was conducted in the absence of any commercial or financial relationships that could be construed as a potential conflict of interest.

References

1. Balsitis SJ, Williams KL, Lachica R, Flores D, Kyle JL, Mehlhop E, Johnson S, Diamond MS, Beatty PR, Harris E (2010) Lethal antibody enhancement of dengue disease in mice is prevented by Fc modification. PLoS Pathog 6:e1000790
2. Beaumier CM, Mathew A, Bashyam HS, Rothman AL (2008) Cross-reactive memory CD8(+) T cells alter the immune response to heterologous secondary dengue virus infections in mice in a sequence-specific manner. J Infect Dis 197:608–617
3. Beaumier CM, Rothman AL (2009) Cross-reactive memory CD4+ T cells alter the CD8+ T-cell response to heterologous secondary dengue virus infections in mice in a sequence-specific manner. Viral Immunol 22:215–219
4. Beaumier CM, Jaiswal S, West KY, Friberg H, Mathew A, Rothman AL (2010) Differential in vivo clearance and response to secondary heterologous infections by H2(b)-restricted dengue virus-specific CD8+ T cells. Viral Immunol 23:477–485
5. Fadilah SA, Sahrir S, Raymond AA, Cheong SK, Aziz JA, Sivagengei K (1999) Quantitation of T lymphocyte subsets helps to distinguish dengue hemorrhagic fever from classic dengue fever during the acute febrile stage. Southeast Asian J Trop Med Public Health 30:710–717
6. Goncalvez AP, Engle RE, St Claire M, Purcell RH, Lai CJ (2007) Monoclonal antibody-mediated enhancement of dengue virus infection in vitro and in vivo and strategies for prevention. Proc Natl Acad Sci USA 104:9422–9427
7. Green S, Pichyangkul S, Vaughn DW, Kalayanarooj S, Nimmannitya S, Nisalak A, Kurane I, Rothman AL, Ennis FA (1999) Early CD69 expression on peripheral blood lymphocytes from children with dengue hemorrhagic fever. J Infect Dis 180: 1429–1435
8. Green S, Vaughn DW, Kalayanarooj S, Nimmannitya S, Suntayakorn S, Nisalak A, Lew R, Innis BL, Kurane I, Rothman AL, Ennis FA (1999) Early immune activation in acute dengue illness is related to development of plasma leakage and disease severity. J Infect Dis 179:755–762
9. Gupta S, Gollapudi S (2008) CD95-mediated apoptosis in naive, central and effector memory subsets of CD4+ and CD8+ T cells in aged humans. Exp Gerontol 43:266–274
10. Guzman MG, Alvarez M, Rodriguez-Roche R, Bernardo L, Montes T, Vazquez S, Morier L, Alvarez A, Gould EA, Kouri G, Halstead SB (2007) Neutralizing antibodies after infection with dengue 1 virus. Emerg Infect Dis 13:282–286
11. Halstead SB (1979) In vivo enhancement of dengue virus infection in rhesus monkeys by passively transferred antibody. J Infect Dis 140:527–533
12. Halstead SB (2007) Dengue. Lancet 370:1644–1652
13. Henchal EA, Henchal LS, Schlesinger JJ (1988) Synergistic interactions of anti-NS1 monoclonal antibodies protect passively immunized mice from lethal challenge with dengue 2 virus. J Gen Virol 69(Pt 8):2101–2107
14. Hus I, Staroslawska E, Bojarska-Junak A, Dobrzynska-Rutkowska A, Surdacka A, Wdowiak P, Wasiak M, Kusz M, Twardosz A, Dmoszynska A, Rolinski J (2011) CD3+/CD16+CD56+ cell numbers in peripheral blood are correlated with higher tumor burden in patients with diffuse large B-cell lymphoma. Folia Histochem Cytobiol 49:183–187
15. Kaufman BM, Summers PL, Dubois DR, Eckels KH (1987) Monoclonal antibodies against dengue 2 virus E-glycoprotein protect mice against lethal dengue infection. Am J Trop Med Hyg 36:427–434
16. Kaufman BM, Summers PL, Dubois DR, Cohen WH, Gentry MK, Timchak RL, Burke DS, Eckels KH (1989) Monoclonal